# Hemostasis defects underlying the hemorrhagic syndrome caused by Mammarenaviruses in a cynomolgus macaque model

Blaise Lafoux, Nicolas Baillet, Caroline Picard, Gustave Fourcaud, Virginie Borges-Cardoso, Stéphanie Reynard, Alexandra Journeaux, Clara Germain, Emeline Perthame, Mathieu Mateo, et al.

# Hemostasis defects underlying the hemorrhagic syndrome caused by Mammarenaviruses in a cynomolgus macaque model

## Short title: Hemostasis defects caused by hemorrhagic fever viruses

Blaise Lafoux[1,2], Nicolas Baillet[1,2], Caroline Picard[1,2], Gustave Fourcaud[1,2], Virginie Borges-Cardoso[1,2], Stéphanie Reynard[1,2], Alexandra Journeaux[1,2], Clara Germain[1,2], Emeline Perthame[3], Mathieu Mateo[1,2], Jimmy Hortion[1,2], Xavier Carnec[1,2], Natalia Pietrosemoli[3], Marie Moroso[4], Orianne Lacroix[4], Ophélie Jourjon[4], Stéphane Barron[4], Audrey Vallve[4], Aurélie Duthey[4], Frédéric Jacquot[4], Laura Barrot[4], Manon Dirheimer[4], Hervé Raoul[4], Christophe Nougier[5], Sylvain Baize[1,2].

[1] Unité de Biologie des Infections Virales Emergentes, Institut Pasteur, Lyon, France.

[2] Centre International de Recherche en Infectiologie (CIRI), Université de Lyon, INSERM U1111, Ecole Normale Supérieure de Lyon, Université Lyon 1, CNRS UMR5308, Lyon France.

[3] Institut Pasteur, Université Paris Cité, Bioinformatics and Biostatistics Hub, F-75015 Paris, France

[4] Laboratoire P4 INSERM-Jean Mérieux, INSERM US003, 69007 Lyon, France.

[5] Service d'hématologie biologique CBPE, Groupement Hospitalier Est, Hospices Civils de Lyon, Bron, France.

Corresponding author: Sylvain Baize, sylvain.baize@pasteur.fr, +33437282443

Main text: 4497 words

Abstract: 218 words

2 tables, 7 figures and 4 supplementary figures

44 references

## Key Points

- Primary and secondary hemostasis defects as well as increased vascular permeability induce a severe hemorrhagic syndrome during arenavirus lethal infection.

## Abstract

Viral hemorrhagic fevers (HF) are a group of acute febrile diseases with high mortality rates. While hemostatic dysfunction appears to be a major determinant of the severity of the disease, it is still unclear what pathogenic mechanisms lead to it. In clinical studies, arenaviruses such as Lassa, Machupo and Guanarito viruses caused HF that vary in symptoms and biological alterations.

In this study we aimed to characterize the hemostatic dysfunction induced by arenaviral HF to determine its implication in the severity of the disease and to elucidate the origin of this syndrome.

We found that lethal infection with Machupo, Guanarito and Lassa viruses is associated with cutaneo-mucosal, cerebral, digestive and pulmonary hemorrhages. The affected animals developed a severe alteration of the coagulation system, which was concomitant with acute hepatitis, minor deficit of hepatic factor synthesis, presence of a plasmatic inhibitor of coagulation and dysfunction of the fibrinolytic system. Despite signs of increased vascular permeability, endothelial cell infection was not a determinant factor of the hemorrhagic syndrome. There were also alterations of the primary hemostasis during lethal infection, with moderate to severe thrombocytopenia and platelet dysfunction. Finally, we show that lethal infection is accompanied by a reduced hematopoietic potential of the bone marrow. This study provides an unprecedented characterization of the hemostasis defects induced by several highly pathogenic Arenaviruses.

## Introduction

The Arenaviridae family comprises several highly pathogenic viruses responsible for hemorrhagic fevers (HF) with high lethality rates [1–3]. Neither vaccine nor treatment has yet been licensed for these diseases [4]. Pathogenic arenaviruses belong to two serotypes, Old World (OW) arenaviruses such as Lassa (LASV), which is endemic to West Africa, and New World (NW) arenaviruses like Machupo (MACV) or Guanarito (GTOV) viruses, which cause epidemics in South America.

Severe arenaviral HF causes neurological and hemorrhagic symptoms that ultimately lead to multi-organ failure, shock syndrome and death. The pathophysiology of these diseases is still largely unknown due to the difficulty of accessing human samples and the necessity of working under BSL-4 conditions. As highlighted by recent publications [5–7], the only animal models that reliably reproduce clinical features of human disease are non-human primates (NHP), which further restricts the number of facilities that can perform such studies.

The hemorrhagic syndrome is a major determinant of the severity of the disease in infected patients. Indeed, clinical bleeding is the symptom most predictive of a death in Lassa fever patients [8]. Additionally, clinical studies have highlighted biomarkers of dysregulated coagulation as strongly predictive of a fatal outcome [9,10]. Thrombocytopenia and platelet dysfunction were demonstrated in fatal cases caused by different arenaviral species, with variable degrees of severity [9–12]. Coagulation tests of activated partial thromboplastin time (aPTT), prothrombin time (PT) and thrombin time (TT) were inconstantly affected in NHP and clinical studies on MACV, JUNV and LASV [13–15].

Infection of vascular endothelial cells (vEC) by arenaviruses is suspected to play a major role in the increased vascular permeability [19,20]. Indeed, vEC can be productively infected *in vitro* by LASV and JUNV [21,22]. These models revealed that infection of vEC induced cellular dysfunction characterized by overexpression of vasoactive agents and adhesion molecules[21,23]. Two studies showed that infection of vEC by JUNV and PICV induced an increase in permeability of vascular monolayers through adherens junction disruption [24,25].

The description and pathophysiology of this complex biological and clinical syndrome is still very fragmented. Notably, no comparative *in vivo* study has ever been done to clarify the link between this hemostasis defect and the severity of the disease, or to compare its extent between arenaviral species. Here we took advantage of a large cohort of animals, which were infected by several arenaviruses and longitudinally monitored in comparable manners to propose a comprehensive analysis of this hemorrhagic syndrome. This animal model reliably reproduced alterations observed in patients and allowed us to study every aspect previously mentioned in the literature to identify differences between viral species and severity factors.

## Methods

1. Study design

All biological samples used for this work were generated during anterior animal studies. The data from a total of 6 separate cohorts of cynomolgus macaques were used. Animals were challenged with viruses diluted between 1,000 and 3,000 FFU/mL of PBS and mock-infected animals were injected with 0.5mL of PBS. These studies took place in a biosafety level 4 (BSL-4) laboratory (Laboratoire P4 Jean Mérieux, France). Details of the follow-up and specimens taken can be found in the original articles [5,6,26,27]. Humane endpoints to the protocol included reaching the maximum clinical score, severe hypothermia, body temperature > 41.5°C for three days, coma or seizure.

2. Viruses

LASV strains AV and Josiah, MACV strain Carvallo and GTOV strain INH-95551 were produced in VeroE6 cells cultured in Dulbecco's Modified Eagle Medium (DMEM). Supernatants were harvested, titrated and frozen at -80°C.

3. Hematology and platelet function tests

Blood collected in EDTA tubes was used to obtain blood cell counts on an MS9 automate (Melet Schloesing Laboratoires). Impedance platelet aggregometry was measured with a Multiplate Analyzer (Roche Diagnostics). Briefly, platelet aggregation in the test plasma was stimulated by four different agonists: adenosine diphosphate (ADP; 6.5µM), ristocetin (RISTO; 0.8mg/mL) and collagen (COL; 3.2µg/mL).

4. Coagulation tests and coagulation factors assays

For coagulation tests such as aPTT, PT, TT and dRVVT as well as fibrinogen and D-Dimer quantifications, plasma was used on a Helena C-4 coagulometer (Helena Biosciences) according to the manufacturer's instructions. Coagulation factors were quantified by proxy of their coagulative potential in cryopreserved plasma from 3.2% sodium citrate tubes for animals infected with LASV AV and LASV Josiah and from EDTA tubes for animals infected with MACV and GTOV. For mixing studies and dRVVT, the control plasma was a pool of 3 mock-infected animals.

5. Colony-forming cells (CFC) assays

Bone marrow mononuclear cells were isolated by centrifugation from aspirates taken at the autopsy. CD34+ cells were immuno-magnetically separated on MACS columns (Miltenyi Biotec) and cultured in semi-solid medium for 10 days at a density of $3.3 \times 10^3$ cells/mL in triplicates. Colony numbers were visually assessed under a light microscope.

6. Histology

Organs were embedded in paraffin. Sections of 3µm of thickness were cut to be stained with hematoxylin and eosin. In situ hybridization was performed with RNAscope (Bio Techne) multiplex kit. Probes were designed to target the S segment of the relevant arenavirus. Immunofluorescence (IF) was done with the following primary antibodies: mouse anti-tissue factor (clone TF9-10H10), rabbit anti-CD31 (clone EP3095) and mouse anti-fibrin (clone 59D8). Detection of viral genome and target proteins was performed with Opal fluorophores (Akoya) and counterstained with DAPI. Images were captured on a LSM980 microscope using the ZEN software (Zeiss). For quantifications, whole-slide images were captured with a Yokogawa CQ1 microscope and analyzed with QuPath software.

7. Human Umbilical Endothelial Vein Cells (HUVEC) and VeroE6 replication kinetics

HUVEC were obtained from three donors and cultured using the E Cell Growth Medium 2 (Promo Cell). Vero E6 cells were used as positive control for infection and grown in DMEM. Cells were infected at a multiplicity of infection of 0.01 and supernatants were harvested at 0, 24, 48, 72 and 96 hours post infection. Titrations were performed on VeroE6 cells.

8. Plasminogen activator inhibitor 1 (PAI-1) ELISA

Cryopreserved plasma sampled at 12 days post-infection was analyzed using PAI-1 monkey ELISA kit from ThermoFisher according to the manufacturer's instructions and read by chemiluminescence on a Tecan Infinite 200 Pro.

9. Western Blots

Lung samples of animals infected with MACV, GTOV or mock-infected were lysed in RIPA buffer (10mg of tissue for 100µL of buffer) using a Qiagen TissueLyser II. Cryopreserved plasma sampled at 12 days post-infection was depleted of albumin and immunoglobulins using HighSelect columns (ThermoFisher). Samples were separated in SDS-PAGE (4-15%) and transferred to a nitrocellulose membrane. Because experimental conditions can modify the overall concentration of proteins in the plasma (via liver deficiency as previously observed [5]) and in the lung (via alveolar edema), we did not normalize sample loading according to protein quantity but rather using a constant weight / volume ratio for the lung and a constant volume of plasma. Target proteins were detected with the following primary antibodies: TF9-10H10 anti-TF, R&D #AF-2974 anti-TFPI, Abcam #ab49735 anti-PF4, Invitrogen #PA5-87043 anti-CD62P, EPR24639-3 anti-ICAM1, EPR5047 anti-VCAM1. Species-specific secondary antibodies conjugated with HRP were used, stainings were performed with Bio-Rad Clarity Max substrate and imaged on an ImageQuant LAS4000. Relative protein levels were evaluated by measuring signal intensities on ImageJ and comparing them with the mean of the three mock animals.

10. Transcriptome

For both RNA-seq datasets, bioinformatics analysis was performed using the RNA-seq pipeline from RNAflow (https://gitlab.pasteur.fr/hub/rnaflow). Reads were cleaned of adapter sequences and low-quality sequences using cutadapt. STAR, with default parameters, was used for alignment against the reference genome. Reads were assigned to genes using featureCounts from the Subreads package. Differential analysis was performed using the DESeq2 R package to identify genes for which the expression profiles were significantly different between each pair of biological conditions.

11. Statistics

An unpaired, non-parametric two-tailed Mann-Whitney t-test was used to compare coagulation parameters, coagulation factor levels, infectious titers in HUVEC, platelet counts, platelet aggregation levels and PAI-1 levels between two groups and an unpaired, parametric Welch's t-test was used to compare colony numbers for CFC assays. For the gene-set related heatmaps, VST transformed data were centered to the Mock and scaled to the variance of each dataset. Then, these normalized datasets were aggregated by condition to obtain one single value by condition and time-point. The sex of the animals was not adjusted for because of the statistical confounding effects of the experimental conditions of interest. For the correlation analysis, AUC was calculated with a baseline of 0 for IFN-α1 and of 281 G/L (the mean of all animals at 0 DPI) for platelets and Pearson's correlation coefficients were calculated.

12. Data Sharing Statement

For original data, please contact the corresponding author.

## Results

A total of 39 cynomolgus macaques were inoculated with pathogenic arenaviruses in a BSL-4 laboratory. Two strains of the Old-World arenavirus LASV, Josiah and AV, were used to challenge respectively 15 and 9 monkeys, while two species of New World Arenaviruses, MACV and GTOV were inoculated to 6 and 3 animals respectively (Suppl Table 1). Three animals served as mock-infected controls.

Infected animals presented a transient leukopenia affecting lymphocytes, monocytes and neutrophils as well as moderate anemia (Suppl Table 2). After a period of non-specific febrile syndrome, AV-infected animals started recovering, while others displayed hemorrhagic symptoms, more commonly in MACV- and GTOV-infected macaques (83% and 100%) than among LASV Josiah animals (55%). Only superficial bleeding such as epistaxis and petechiae were noted for the latter, while MACV- and GTOV-infected groups developed digestive tract hemorrhages manifested by melena and hematochezia. All animals infected with LASV Josiah or MACV and one GTOV animal were euthanized between 11 and 18 days post-infection (DPI) because they reached the clinical endpoint. One GTOV and all LASV AV animals started recovering after 18-20 DPI while the third GTOV-infected displayed symptoms until the end of the procedure.

Necropsies revealed gross pathological lesions in animals that succumbed to infection (Suppl Table 1 and Suppl Figure 1). Macaques fatally infected with LASV Josiah, MACV and GTOV presented hemorrhages in the lungs, gastro-intestinal tract and intracranial space. All animals presented peritoneal effusions, indicating increased vascular permeability.

Organs harvested at autopsy were stained in hematoxylin and eosin and examined microscopically to determine the localization and the eventual cause of bleeding.

The lungs of animals infected with MACV, GTOV and LASV Josiah presented histopathologic features of acute lung injury (Figure 1, left column). Parietal thickening due to immune cells infiltration was found in lethally infected animals. These animals had areas of hemorrhage in the lung parenchyma. A large number of hemosiderin-laden macrophages was present, indicating an active hemophagocytosis. Alveolar edema was also observed, predominantly in LASV Josiah animals. The absence of capillary congestion did not point toward cardiogenic edema but rather increased vascular permeability.

The most frequent lesions across all lethally infected animals were found in the liver, evocating an acute viral hepatitis (Figure 1, right column). The presence of peri-portal mononuclear cells infiltrates was noted in all studied animals, with LASV Josiah and MACV animals presenting the most severe form. Hepatocellular damage was also overt, in various extent between groups. GTOV-infected animals presented the mildest form, with the presence of swollen hepatocytes and diffuse Councilman apoptotic bodies. One LASV Josiah and two MACV-infected monkeys had severe lesions with numerous apoptotic bodies, focal necrosis of hepatocytes and ballooning degeneration of large areas. Lobular organization was perturbed among all groups, manifested by congested sinusoids and loss of visible demarcation between lobules. All LASV AV-infected animals were exempt of any pathological change at the time of euthanasia.

We investigated the coagulation parameters of infected cynomolgus macaques to determine whether clinical bleeding was related to specific alterations of hemostasis. The aPTT was significantly prolonged for MACV and GTOV animals at 8 DPI and continued increasing until death for MACV while it returned to almost normal values for GTOV at 12 DPI (Figure 2A). For LASV Josiah-infected monkeys, aPTT prolongation started as soon as at 4 DPI and continuously increased until death while it stayed close to normal for LASV AV animals. PT was prolonged in MACV-infected animals from 4 DPI to 12 DPI with

a peak at 8 DPI, time point at which the PT of GTOV animals was also prolonged before going back towards normal values (Figure 2B). Among the LASV Josiah group, the increase was slightly slower but followed a similar pattern with a peak at 8 DPI while LASV AV animals remained normal throughout the study.

Plasma fibrinogen levels steadily increased starting at 4 DPI and until 12 DPI in all groups (Figure 2C). D-dimers levels remained low except for two outlier animals in MACV and GTOV groups that were transiently increased but came back to normal by 8 DPI (Figure 2D). In MACV- but not GTOV-infected animals, thrombin time (TT) showed a late prolongation at 12 DPI, while in LASV Josiah animals it was strongly elevated from 8 DPI (Figure 2E).

To determine whether the alterations of coagulation could be explained by a dysfunction of hepatocytes during infection, we conducted a transcriptomic analysis of liver cells from animals infected with LASV Josiah, LASV AV and MACV. Total RNA was extracted from organs harvested at three sequential points of euthanasia, 2, 5 and 11 DPI for the two LASV strains or when animals reached the clinical endpoint for MACV. The expression of three publicly available gene sets was compared to the mock-infected animals (Figure 3A). Gene expression of factors XII, XI and VII was significantly downregulated in Josiah and MACV animals at 11 DPI, while factors V, IX and X showed little to no change (Suppl figure 2). Consistent with the observed hyperfibrinogemia, the genes encoding two of the fibrinogen subunits, FGB and FGG, were upregulated in the Josiah group at 11 DPI. The KLKB1 gene coding for plasma kallikrein and the KNG1 gene coding for kininogen, two pro-coagulant proteins were also down-regulated during lethal infection. The fibrinolysis system appeared to be negatively impacted in animals developing a severe disease. Indeed, the expression of key inhibitors of fibrinolysis SERPINE1 (also known as PAI-1), TIMP1 and HRG was increased in Josiah animals at 11 DPI and MACV at the time of death while PLG, which encodes for plasminogen was decreased. The overall expression level of these gene sets was compared between infected and mock-infected groups (Figure 3B). The expression of the Coagulation gene set was significantly lower in the Josiah 5 DPI group and the Clotting cascade gene set was down-regulated in Josiah 5 DPI, Josiah 11 DPI and MACV groups, indicating that hepatocyte dysfunction in lethal infection can play a role in dysregulated hemostasis.

We measured the activity of coagulation factors to determine if secondary hemostasis defects could be due to a decreased coagulation factor synthesis (Figure 4A and 4B). During the course of the disease, the activity of FXI, FIX, FVIII and FVII decreased for MACV and GTOV animals. LASV-infected animals also presented alterations of FXII, FXI, FVIII and FVII but did not strongly differ between AV and Josiah strains. Importantly, all factors remained higher than 60% of their normal activity.

To investigate the anti-coagulant activity of infected plasma, we performed a mixing test on plasma from Josiah-infected animals at 8 and 11 DPI (Figure 5A). The Rosner index was calculated for each sample to determine if the mix of the infected plasma and the control plasma had a corrected coagulation time. At 8 DPI, 6 animals out of 9 had a prolonged aPTT and all of them had a Rosner index >10, indicating the presence of a plasmatic inhibitor of coagulation. At 11 DPI, all 9 animals had both prolonged aPTT and a Rosner >10. Because lupus anticoagulants (LA) are commonly observed in viral infections[28] we performed a dRVVT test on these plasma (Figure 5B). None of the 18 samples tested had a prolonged dRVVT, indicating that LA was not the cause of the observed coagulopathy.

To determine if direct infection of endothelial cells was responsible for the observed increased vascular permeability, we performed multiplexed immunofluorescence on the tissues of infected animals (Figure 6A). We used RNA in situ hybridization (ISH) to detect viral genome and IF for the endothelial cell marker CD31, fibrin and tissue factor (TF). Co-localization of ISH and CD31 was observed in LASV Josiah but not GTOV- or MACV-infected animals (Figure 6A and Suppl figure 3A) and TF staining was

more pronounced on the vessel walls in animals infected with MACV, GTOV and LASV Josiah. To quantitatively measure vEC infection, we performed whole-organ confocal scanning of the lungs, individual cell detection and classification according to CD31 and/or vRNA positivity (Figure 6B), which confirmed that LASV Josiah had more tropism for vEC than the other viral strains (Figure 6C). In the kidneys and lungs of Josiah animals, we found a large number of fibrin-obstructed capillaries and areas of fibrin deposits along the alveolar walls. We measured the plasma levels of PAI-1 at the peak of the disease and found significant differences to the mock condition for animals infected by LASV Josiah or MACV. We used another immunofluorescence panel coupling ISH, TF and the monocytic marker CD68 (Supplementary figure 3B) which showed that monocytes containing viral RNA of LASV Josiah, MACV and GTOV displayed abnormal TF expression. Western Blot analysis of lung homogenates (Supplementary Figures 3D and 3E) revealed increased levels of TF in all infected conditions except GTOV and increased TFPI in all conditions compared to the mock. We also studied the replication of LASV Josiah, MACV and GTOV in human umbilical vascular endothelial cells (HUVEC) (Fig 6D). LASV Josiah had a faster growth curve and reached a higher peak at 3 DPI than MACV and GTOV which reached their peak at 4 DPI. Notably, there was a total absence of GTOV replication in two of the three tested donors of HUVEC. To study vEC activation, we measured ICAM-1 and VCAM-1 levels in lung samples (Supplementary Figures 3F and 3G), which showed increased expression following viral challenge especially in Josiah and MACV groups. These results indicate that tropism of arenaviruses for vEC is not the main cause of the observed hemorrhagic tendency, at least in the case of NW arenaviruses MACV and GTOV.

To compare the kinetics and amplitude of thrombocytopenia between different arenaviral HF, we measured platelet counts after challenge. GTOV-infected animals had a transient and moderate thrombocytopenia, peaking at 8 DPI (Figure 7A). On the other hand, the MACV group presented a more severe form, reaching its lowest at 11 DPI with a mean of 31 G/L. LASV AV and Josiah infected monkeys had similar patterns up to 12 DPI when the AV group started to recover and Josiah kept decreasing until death (Figure 7B). Because high levels of type-I IFN can cause thrombocytopenia[29], we performed a correlation analysis between IFN-α1 levels and platelet counts indiscriminately of viral species but found no significant correlation (Suppl Figure 4A).

To test platelet function, we measured aggregation in response to different agonists (Figure 7B). LASV Josiah and GTOV but not MACV-infected animals presented lower ratios of aggregation per platelet than non-infected controls in response to ADP, ristocetin and collagen. Additionally, we found largely increased levels of soluble PF4 in the plasma of animals infected with Josiah and GTOV compared to the mock (Supplementary Figures 4B and 4C).

To determine if thrombocytopenia might be due to a defect in hematopoiesis, we isolated CD34+ hematopoietic cells from the bone marrow of animals infected with LASV Josiah and previously vaccinated with MeV-LASV or not. This vaccine protected 100% of animals against a lethal challenge from LASV Josiah with minimal and transient clinical signs [27]. We performed colony-forming cells assays on these samples and quantified lineage-restricted progenitors after 10 days of culture (Figure 7D). There was an overall decrease in the ability of CD34+ cells from non-vaccinated animals to differentiate into hematopoietic progenitors, except for their most immature form, CFU-GEMM. The erythroid lineage was particularly affected, while monocytic-granulocytic lineages were slightly increased in relative frequency. This indicates that lethal LASV Josiah infection is associated with defective hematopoietic differentiation and proliferation.

## Discussion

Despite their clear implication in disease severity, the understanding of hemostasis defects associated with arenaviral HF remained unclear. In this study, we present the first comparative analysis of hemostatic disorders induced by four highly pathogenic Arenaviruses in a NHP model.

Following the principle of reducing the number of animals used to reach a scientific aim, we took advantage of non-vaccinated animals that were initially part of multiple vaccine studies. This design introduces heterogeneity in the material available for each group. To minimize the bias associated to separate animal experiments, we matched infected groups to relevant control groups for which we had comparable samples in all experiments, allowing robust comparisons.

Our model of infection recapitulated all the hematological features observed in clinical studies: thrombocytopenia, leukopenia, platelet dysfunction, clotting time prolongation, high PAI-1 levels and hemorrhagic symptoms [8,10–12,30–33]. The differences in the severity of these features between the AV and Josiah strains also recapitulate the discrepancies observed between severe and mild Lassa fever patients.

Because the cutaneo-mucosal bleeding observed in patients is usually limited, it was uncertain whether the hemorrhagic syndrome could really be implicated in the disease severity. We identify for the first time that arenavirus infection can induce cerebral and cerebellar hemorrhages. These hemorrhages can cause coma and death by infarction or compression of the central nervous system. Increased permeability highlighted by peritoneal effusions and pulmonary edema could also play a role in the terminal shock syndrome by inducing fluid balance dysregulation, tissue hypoxia and multi-organ failure as observed in fatal cases [34].

We set out to determine the underlying causes of hemorrhages by first investigating the coagulation system. Clotting times were prolonged in all lethally infected animals despite an absence of consumption coagulopathy via DIC, as evidenced by elevated fibrinogen, close to normal levels of coagulation factors and the absence of D-dimers. This is in accordance with data obtained in infected patients in which thrombocytopenia is moderate and levels of fibrin degradation products are not correlated with outcome [9,32].Because this coagulopathy was accompanied by severe tissue damage, infiltration of immune cells, degeneration of hepatocytes in the liver and elevated hepatic enzymes [5,6] we performed a transcriptomic analysis of liver cells to investigate a potential link. In lethally infected monkeys, there was indeed a down-regulation of coagulation factors transcription as well as that of coagulation system proteins such as kininogen and kallikrein and an up-regulation of inhibitors of fibrinolysis. Despite these indications of liver damage involvement in the coagulopathy, the activity of coagulation factors in the plasma was only moderately lowered and did not reach levels that could cause clotting time prolongation or bleeding on its own. Consequently, we performed plasma-mixing experiments that showed the presence of a circulating inhibitor of coagulation in the plasma of animals infected with Josiah. We could not identify this inhibitor but we propose several possible causes: (1) an endogenous heparin-like substance over-expressed during the infection or (2) a secreted viral protein such as GP1 [35,36]. Interestingly, it has been reported that platelet dysfunction may also be mediated by a soluble factor, which could be the same as the one we identified [11,12]. If so, antagonizing the activity of this factor would have a great therapeutic potential.

Our histological analysis showed that infection with LASV Josiah resulted in fibrin deposition in the lungs and kidneys. Because vessel walls and infected monocytes displayed increased staining for TF antigen, we suspected that resulted from a local thrombogenic environment but TF / TFPI levels measured in the lungs by Western Blot were not correlated to the presence of fibrin. Topologically, TF

staining on vessel walls was not predictive of fibrin deposition on the surrounding tissue. Plasma levels of the anti-fibrinolytic protein PAI-1 were not higher in LASV Josiah animals either. Other actors such as the complement and kinin systems may be activated by local inflammation and result in a loss of balance between pro-coagulant and fibrinolytic activities.

Many studies hypothesized that direct infection of vEC was the cause of increased vascular permeability. We show that NW arenaviruses MACV and GTOV, which caused peritoneal effusions and lung edema, have very little *in vivo* tropism for endothelial cells and that they replicate less efficiently than LASV Josiah in human primary endothelial cells. This indicates that tropism for vEC is not the determining factor in the increased vascular permeability caused by these viruses, although it may be implicated in the case of LASV Josiah. On the other hand, it is possible that the release of inflammatory mediators such as IL-6 and TNF-α (which is described in this model [5]) by activated immune cells causes vEC activation as highlighted by ICAM-1 and VCAM-1 upregulation. Additionally, activated EC are known to produce increased levels of PAI-1[37], which is a feature of infection by LASV Josiah and MACV. This activation can result in a loss of barrier integrity which leads to vascular leakage and increased leukocyte extravasation resulting in leukopenia and immune cell infiltration, both of which observed in our model. Importantly, this process is not dependent on direct infection of vEC but rather on the immunological state of the host, explaining the presence of these signs in animals infected with NW arenaviruses.

We show that arenaviral HF is accompanied by a central hematopoiesis defect that could be responsible for the observed thrombocytopenia. Moreover, studies of the Lymphocytic Choriomeningitis virus (LCMV) showed that IFN signaling may induce a deficit in platelet production and serotonin release during infection [38,39]. This mechanism could also be suspected for HF-causing arenaviruses as they induce a strong release of IFN in the blood stream [40] but our correlation analysis showed no significant link between IFN-α1 levels and platelet counts. In addition to low platelet counts, animals infected with GTOV and LASV Josiah but not MACV presented an acquired platelet dysfunction. As previously mentioned, evidence shows that this platelet dysfunction may be mediated by a soluble factor in the plasma of the infected host [11,12,30]. Notably, most described inhibitors of platelet aggregation are not able to antagonize ADP, ristocetin and collagen induced responses simultaneously. Our study suggests 2 non-exclusive mechanisms for this syndrome: (1) activated vEC release pathological levels of ADPases, prostacyclin and nitric oxide that have anti-aggregatory effects and (2) overt platelet activation suggested by high levels of soluble PF4 results in platelet exhaustion as described elsewhere [41–43].

Finally, some aspects of the pathology such as increased PAI-1 expression, fibrin deposition, low FVII levels and expression of TF on monocytes that are reminiscent of sepsis-associated hemostatic disorders, which could represent an incentive to translating some therapeutic interventions already used successfully in sepsis patients [44].

To summarize, we provide evidence that during arenaviral infection, potentially life-threatening bleeding are associated with hepatic failure and coagulopathy mediated by a circulating inhibitor of coagulation. These symptoms do not appear to be related to vEC infection but rather to endothelium activation. Simultaneously, decreased hematopoietic activity, thrombocytopenia and platelet aggregation defects impair primary hemostasis, participating to the hemorrhagic syndrome. These findings will allow better understanding of hemorrhagic fever syndromes caused by arenaviruses but also viruses such as Ebola, Dengue and Yellow Fever. It also provides a framework to test potential therapeutics and countermeasures to this syndrome.

## Acknowledgements

We thank S. Prost (CEA, Université Paris Sud 11, INSERM U1184, IDMIT Department, Fontenay-aux-Roses, France) for his advices and help in studying hematopoiesis. We thank G. Jouvion (Ecole Nationale Vétérinaire d'Alfort, Unité d'Histologie et d'Anatomie Pathologique, Maisons-Alfort, France) for advices on anatomic pathology. We are grateful to K. Noy (UBIVE) for his assistance in the writing process. We thank J. Brocard, E. Chatre and E. Caracas Bobocioiu (PLATIM, SFR Biosciences, UAR3444/CNRS, US8/Inserm, ENS de Lyon, UCBL) for their assistance in the development of spectral confocal microscopy. We thank Q. Pascal and S. Luccantoni (CEA, Université Paris Sud 11, INSERM U1184, IDMIT Department, Fontenay-aux-Roses, France) for their advices on tissue processing and staining. We are grateful to B. Renaudin (UBIVE) for her administrative support. This study was funded by the Délégation Générale pour l'Armement (Agence Nationale de la Recherche - Accompagnement Spécifique des Travaux de Recherches et d'Innovation Défense, ANR-ASTRID 2014, France) and by a grant from the "Grand Projet Fédérateur de Vaccinologie" of the Institut Pasteur obtained by S. Baize.

## Authors' contribution

S. Baize, S.R., M. Mateo and N.B. designed the animal experiments. M. Moroso, O.L., O.J., S. Barron, A.V., A.D. and F.J. handled the animal care and autopsies. N.B., J.H., G.F. and B.L. processed the tissues. B.L. did the H&E staining and imaging, multiplex IF staining and imaging and CFC assays. C.P., V.B-C. and S.R. did the coagulation and platelet function tests. C.P. and B.L. performed the coagulation factors tests. E.P. did the transcriptomic analysis. G.F. did the experiments on HUVECs and extractions of RNA for MACV animals. N.B., C.P., S.R., M. Mateo, V.B-C., A.J, C.G. and X.C participated in bone marrow specimens processing and hematologic counts. B.L. analyzed the data. S. Baize and B.L. wrote the paper. C.N. reviewed the paper. S. Baize supervised the project.

## Disclosure of Conflicts of Interest

The authors state no competing interests.

## References


1. Carey DE, Kemp GE, White HA, et al. Lassa fever. Epidemiological aspects of the 1970 epidemic, Jos, Nigeria. *Trans R Soc Trop Med Hyg*. 1972;66(3):402-408. doi:10.1016/0035-9203(72)90271-4

2. Monath TP, Mertens PE, Patton R, et al. A hospital epidemic of Lassa fever in Zorzor, Liberia, March-April 1972. *Am J Trop Med Hyg*. 1973;22(6):773-779. doi:10.4269/ajtmh.1973.22.773

3. Bowen GS, Tomori O, Wulff H, Casals J, Noonan A, Downs WG. Lassa fever in Onitsha, East Central State, Nigeria in 1974. *Bull World Health Organ*. 1975;52(4-6):599-604.

4. Cheng HY, French CE, Salam AP, et al. Lack of Evidence for Ribavirin Treatment of Lassa Fever in Systematic Review of Published and Unpublished Studies1. *Emerg Infect Dis*. 2022;28(8):1559-1568. doi:10.3201/eid2808.211787

5. Baillet N, Reynard S, Perthame E, et al. Systemic viral spreading and defective host responses are associated with fatal Lassa fever in macaques. *Commun Biol*. 2021;4(1):27. doi:10.1038/s42003-020-01543-7

6. Reynard S, Carnec X, Picard C, et al. The MOPEVAC vaccine induces humoral responses and sterilizing immunity against New World arenaviruses. *Nature Microbiology*.

7. Hensley L, Smith M, Geisbert J, et al. Pathogenesis of Lassa fever in cynomolgus macaques. *Virol J*. 2011;8:205. doi:10.1186/1743-422X-8-205

8. McCormick JB, King IJ, Webb PA, et al. A case-control study of the clinical diagnosis and course of Lassa fever. *J Infect Dis*. 1987;155(3):445-455. doi:10.1093/infdis/155.3.445

9. Horton LE, Cross RW, Hartnett JN, et al. Endotheliopathy and Platelet Dysfunction as Hallmarks of Fatal Lassa Fever. *Emerg Infect Dis*. 2020;26(11):2625-2637. doi:10.3201/eid2611.191694

10. Fisher-Hoch SP, McCormick JB, Sasso D, Craven RB. Hematologic dysfunction in Lassa fever. *J Med Virol*. 1988;26(2):127-135. doi:10.1002/jmv.1890260204

11. Cummins D, Fisher-Hoch SP, Walshe KJ, et al. A plasma inhibitor of platelet aggregation in patients with Lassa fever. *Br J Haematol*. 1989;72(4):543-548. doi:10.1111/j.1365-2141.1989.tb04321.x

12. Cummins D, Molinas FC, Lerer G, Maiztegui JI, Faint R, Machin SJ. A Plasma Inhibitor of Platelet Aggregation in Patients with Argentine Hemorrhagic Fever. *Am J Trop Med Hyg*. 1990;42(5):470-475. doi:10.4269/ajtmh.1990.42.470

13. Scott SK, Hickman RL, Lang CM, Eddy GA, Hilmas DE, Spertzel RO. Studies of the Coagulation System and Blood Pressure during Experimental Bolivian Hemorrhagic Fever in Rhesus Monkeys. *Am J Trop Med Hyg*. 1978;27(6):1232-1239. doi:10.4269/ajtmh.1978.27.1232

14. Molinas FC, Giavedoni E, Frigerio MJ, Calello MA, Barcat JA, Weissenbacher MC. Alteration of blood coagulation and complement system in neotropical primates infected with Junin virus. *J Med Virol*. 1983;12(4):281-292. doi:10.1002/jmv.1890120408

15. Lange JV, Mitchell SW, McCormick JB, Walker DH, Evatt BL, Ramsey RR. Kinetic Study of Platelets and Fibrinogen in Lassa Virus-Infected Monkeys and Early Pathologic Events in Mopeia Virus-Infected Monkeys. *Am J Trop Med Hyg*. 1985;34(5):999-1007. doi:10.4269/ajtmh.1985.34.999

16. Molinas FC, Paz RA, Rimoldi MT, Bracco MME d. Studies of Blood Coagulation and Pathology in Experimental Infection of Guinea Pigs with Junin Virus. *J Infect Dis*. 1978;137(6):740-746. doi:10.1093/infdis/137.6.740

17. Fisher-Hoch SP, Mitchell SW, Sasso DR, Lange JV, Ramsey R, McCormick JB. Physiological and Immunologic Disturbances Associated with Shock in a Primate Model of Lassa Fever. *J Infect Dis*. 1987;155(3):465-474. doi:10.1093/infdis/155.3.465

18. Stein DR, Warner BM, Audet J, et al. Differential pathogenesis of closely related 2018 Nigerian outbreak clade III Lassa virus isolates. *PLOS Pathog*. 2021;17(10):e1009966. doi:10.1371/journal.ppat.1009966

19. Kunz S. The role of the vascular endothelium in arenavirus haemorrhagic fevers. *Thromb Haemost*. 2009;102(6):1024-1029. doi:10.1160/TH09-06-0357

20. Peters CJ, Zaki SR. Role of the endothelium in viral hemorrhagic fevers. *Crit Care Med*. 2002;30(5 Suppl):S268-273. doi:10.1097/00003246-200205001-00016

21. Lukashevich IS, Maryankova R, Vladyko AS, et al. Lassa and Mopeia Virus Replication in Human Monocytes/Macrophages and in Endothelial Cells: Different Effects on IL-8 and TNF-α Gene Expression. *J Med Virol*. 1999;59(4):552-560.

22. Andrews BS, Theofilopoulos AN, Peters CJ, Loskutoff DJ, Brandt WE, Dixon FJ. Replication of dengue and junin viruses in cultured rabbit and human endothelial cells. *Infect Immun*. 1978;20(3):776-781.

23. Gomez RM, Pozner RG, Lazzari MA, et al. Endothelial cell function alteration after Junin virus infection. *Thromb Haemost*. 2003;90(2):326-333. doi:10.1160/TH02-09-0043

24. Brocato RL, Voss TG. Pichinde virus induces microvascular endothelial cell permeability through the production of nitric oxide. *Virol J*. 2009;6:162. doi:10.1186/1743-422X-6-162

25. Lander HM, Grant AM, Albrecht T, Hill T, Peters CJ. Endothelial Cell Permeability and Adherens Junction Disruption Induced by Junín Virus Infection. *Am J Trop Med Hyg*. 2014;90(6):993-1002. doi:10.4269/ajtmh.13-0382

26. Mateo M, Reynard S, Journeaux A, et al. A single-shot Lassa vaccine induces long-term immunity and protects cynomolgus monkeys against heterologous strains. *Sci Transl Med*. 2021;13(597):eabf6348. doi:10.1126/scitranslmed.abf6348

27. Mateo M, Reynard S, Carnec X, et al. Vaccines inducing immunity to Lassa virus glycoprotein and nucleoprotein protect macaques after a single shot. *Sci Transl Med*. 2019;11(512):eaaw3163. doi:10.1126/scitranslmed.aaw3163

28. Uthman IW, Gharavi AE. Viral infections and antiphospholipid antibodies. *Semin Arthritis Rheum*. 2002;31(4):256-263. doi:10.1053/sarh.2002.28303

29. Rivadeneyra L, Pozner RG, Meiss R, Fondevila C, Gómez RM, Schattner M. Poly (I:C) downregulates platelet production and function through type I interferon. *Thromb Haemost*. 2015;114(11):982-993. doi:10.1160/TH14-11-0951

30. Horton LE, Sullivan BM, Garry RF, et al. Dysfunctional Platelet Aggregation in Patients with Acute Lassa Fever. *Open Forum Infect Dis*. 2017;4(suppl_1):S223. doi:10.1093/ofid/ofx163.460

31. de Manzione N, Salas RA, Paredes H, et al. Venezuelan hemorrhagic fever: clinical and epidemiological studies of 165 cases. *Clin Infect Dis Off Publ Infect Dis Soc Am*. 1998;26(2):308-313. doi:10.1086/516299

32. Strampe J, Asogun DA, Speranza E, et al. Factors associated with progression to death in patients with Lassa fever in Nigeria: an observational study. *Lancet Infect Dis*. 2021;21(6):876-886. doi:10.1016/S1473-3099(20)30737-4

33. Molinas FC, de Bracco MM, Maiztegui JI. Coagulation studies in Argentine hemorrhagic fever. *J Infect Dis*. 1981;143(1):1-6. doi:10.1093/infdis/143.1.1

34. Duvignaud A, Jaspard M, Etafo IC, et al. Lassa fever outcomes and prognostic factors in Nigeria (LASCOPE): a prospective cohort study. *Lancet Glob Health*. 2021;9(4):e469-e478. doi:10.1016/S2214-109X(20)30518-0

35. Branco LM, Grove JN, Moses LM, et al. Shedding of soluble glycoprotein 1 detected during acute Lassa virus infection in human subjects. *Virol J*. 2010;7:306. doi:10.1186/1743-422X-7-306

36. Branco LM, Garry RF. Characterization of the Lassa virus GP1 ectodomain shedding: implications for improved diagnostic platforms. *Virol J*. 2009;6(1):147. doi:10.1186/1743-422X-6-147

37. Hunt BJ, Jurd KM. Endothelial cell activation. *BMJ*. 1998;316(7141):1328-1329.

38. Pozner RG, Ure AE, Jaquenod de Giusti C, et al. Junín virus infection of human hematopoietic progenitors impairs in vitro proplatelet formation and platelet release via a bystander effect involving type I IFN signaling. *PLoS Pathog*. 2010;6(4):e1000847. doi:10.1371/journal.ppat.1000847

39. Aiolfi R, Sitia G, Iannacone M, Brunetta I, Guidotti LG, Ruggeri ZM. Arenaviral infection causes bleeding in mice due to reduced serotonin release from platelets. *Sci Signal*. 2022;15(722):eabb0384. doi:10.1126/scisignal.abb0384

40. Levis SC, Saavedra MC, Ceccoli C, et al. Correlation between endogenous interferon and the clinical evolution of patients with Argentine hemorrhagic fever. *J Interferon Res*. 1985;5(3):383-389. doi:10.1089/jir.1985.5.383

41. Kornblith LZ, Robles AJ, Conroy AS, Miyazawa BY, Callcut RA, Cohen MJ. Tired Platelet: Functional Anergy after Injury. *J Am Coll Surg*. 2017;225(4):S64. doi:10.1016/j.jamcollsurg.2017.07.131

42. Systemic Platelet Exhaustion in Critically-ill Covid-19 Patients. ISTH Congress Abstracts. Accessed July 5, 2023. https://abstracts.isth.org/abstract/systemic-platelet-exhaustion-in-critically-ill-covid-19-patients/

43. Fong JS, Kaplan BS. Impairment of platelet aggregation in hemolytic uremic syndrome: evidence for platelet “exhaustion.” *Blood*. 1982;60(3):564-570.

44. Levi M, van der Poll T. Coagulation and sepsis. *Thromb Res*. 2017;149:38-44. doi:10.1016/j.thromres.2016.11.007

## Figures Legends

**Figure 1. Histopathological changes associated with hemostasis defects in the organs of infected monkeys.** Samples harvested during necropsy of animals infected with MACV, GTOV, LASV Josiah, LASV AV or mock-infected were stained using hematoxylin-eosin coloration. Black squares correspond to the area imaged in the inset on the right. **Left column**: lungs show varying degrees of hemorrhage, alveolar edema and interstitial infiltration. Black arrowheads indicate areas of hemorrhage and white arrowheads indicate alveolar edema. **Right column**: hepatic parenchyma injury includes macrovesicular steatosis, focal necrosis and peri-portal mononuclear infiltrates. Black arrowheads indicate areas of hepatocellular degeneration and necrosis; white arrowheads indicate inflammatory infiltrates. Images are representative of observations made in three different animals for each condition. Left column scale bar = 100µm; right column scale bar = 50µm.

**Figure 2. Coagulation system defects associated with hemorrhagic fever-causing arenaviruses. A.** Activated Partial Thromboplastin Time expressed in seconds. **B.** Prothrombin time expressed in seconds. **C.** Fibrinogen concentration in g/L. **D.** D-Dimers levels in ng/mL. **E.** Thrombin Time expressed in seconds. Mean values for infected animals (MACV in magenta, GTOV in green, LASV AV in blue and LASV Josiah in red) are presented with error bars for SEM. The base value for each parameter is presented as the mean of all values from 3 mock-infected animals and the value at the day of challenge of 24 animals. Continuous black line represents the mean and dotted line the SEM. Asterisks indicate a statistically significant difference with the base level according to a two-tailed Mann-Whitney test (one asterisk for $p<0.05$, two for $p<0.005$ and three for $p<0.0005$). Tests were done for values at 4, 8, 11 and 12 DPI. Number of animals**:** 3 MACV-infected, 3 GTOV-infected animals, 12 LASV Josiah-infected and 6 LASV AV-infected animals.

**Figure 3. Significant transcriptomic changes associated with hemostasis in the liver of macaques infected with LASV Josiah, LASV AV and MACV. A.** Transcriptomic analysis of liver cells at 2, 5 or 11 DPI for AV and Josiah or at time of death for MACV. The heatmaps represent the gene expression in each pathway. Only statistically differentially expressed genes (for Josiah VS Mock, Josiah VS AV or MACV VS Mock comparisons) are included. The color of the heatmaps represents the Mock-related scaled normalized counts averaged for each group and time-point (n=3 for each time point and infection status and n=6 for MACV). Gene names were annotated regarding their differential expression status: asterisk refers to genes significant in the mock-AV-Josiah dataset while degree symbols refers to genes significant in the Machupo dataset. **B.** Violin plots comparing the global expression variation relative to the mock. The overall gene sets over- or under-expression was tested with a 1-way mixed ANOVA and p-values were corrected with the Tukey's multiple comparison test.

**Figure 4. Alterations of coagulation factor activity following arenavirus-induced hemorrhagic fevers. A.** Factors of the intrinsic pathway of coagulation: factors XII, XI, IX and VIII. **B.** Factors of the extrinsic and common pathway: factors II, V, VII and X. Tests were performed using EDTA plasma for GTOV and MACV and citrate plasma for LASV Josiah and AV. Legend is as for figure 2. Base level is calculated as the mean of all values from 3 mock-infected animals and the value at the day of challenge of 6 infected animals. Three animals of each infection status were included.

**Figure 5. Presence of a circulating inhibitor of coagulation in the plasma of LASV Josiah animals**. **A.** Plasma from LASV Josiah infected animals at 8 or 11 DPI was mixed 50:50 with a pool of 3 mock-infected animals. The aPTT of the test plasma, the control plasma and the mixed plasma were measure to calculate the Rosner index as follows: RI = (aPTT of mix - aPTT of control) / aPTT of test. Squares represent the samples for which the aPTT of the test plasma was within a 95% confidence interval of the mean of mocks and circles the samples with a prolonged aPTT. Red bars represent the mean of

each time point. Dashed lines highlight the scores of 10 and 15, between which the result is evocative of an inhibitor of coagulation but inconclusive and above which the test is considered positive with certainty. **B.** Dilute Russel Viper Venom Time (dRVVT) of LASV Josiah infected animals at 8 or 11 DPI. Legend is as previously, except for the dashed line that indicates the score of 1.5, which is the threshold of positivity for lupus anticoagulant.

**Figure 6. Differences in tropism for endothelial cells between hemorrhagic fever-causing arenaviruses. A.** Multiplex immunofluorescence and ISH staining of kidney sections from infected or mock-infected animals. Single channel images of DAPI, CD31 (vascular endothelial cells), fibrin, viral RNA and tissue factor are shown as well as their merge. Images are representative of observations made in three separate animals for each condition. Scale bar corresponds to 50 µm. B. Whole slide images obtained by confocal scanner. Three slices in the Z dimension where transformed by Maximum Intensity Projection. Left image shows a whole lung from a LASV Josiah infected animal with the three stainings merged. The three images in the center correspond to the white inset and allow appreciation of the staining localization at a cellular level. It includes a medium caliber vessel surrounded by alveoli. Scale bars = 50µm. The two images on the right are from QuPath software and illustrate the process of cell detection based on DAPI staining and cell classification based on CD31 and vRNA positivity. Color-coding: blue = unclassified; green = CD31+ vRNA-; yellow = CD31+ vRNA+; red = CD31- vRNA+. C. Quantification of the classification obtained in the previous analysis. Three organs for each condition were quantified. **D.** Infectious particles titers in the supernatant of HUVEC infected with 3 different hemorrhagic fever-causing Arenaviruses, harvested at 5 different time points post-infection. Error bars correspond to the standard error of the mean (SEM) of three replicates, asterisks signal a statistically significant difference between titers at 4 DPI according to a two-tailed Mann-Withney test ($p<0.05$).

**Figure 7. Variable levels of thrombocytopenia and platelet dysfunction during infection with highly pathogenic arenaviruses. A.** Platelet counts expressed in giga cells/L. Base level is calculated as the mean of all values from 3 mock-infected animals and the value at the day of challenge of 53 animals. The rest of the legend is as previously described. **B.** Platelet function evaluated through platelet aggregation normalized by platelet count. Platelet aggregation was measured in response to three classical platelet agonists: adenosine diphosphate (ADP), ristocetin (RISTO) and collagen (COL). Tests were performed at the day of euthanasia and raw values were normalized by the platelet count on the corresponding time point. Bars and error bars represent the mean and SEM of each conditions, individual values appear as circles. Asterisks indicate a statistically significant difference with the base level according to a two-tailed Mann-Whitney test (one asterisk for $p<0.05$, two for $p<0.01$ and three for $p<0.005$). **C.** Number and relative frequency of colonies from each myeloid lineage obtained after a 10 day culture of CD34+ hematopoietic cells from vaccinated and unvaccinated animals challenged with LASV Josiah animals. Bone marrow specimens from three animals in each condition were used and cultures were carried out in triplicates. Dots correspond to the mean of technical triplicates, bars to the mean of three animals and error bars to their S.E.M. Asterisks indicate a statistically significant difference with the base level according to a Welch's t-test (one asterisk for $p<0.05$ and two for $p<0.01$).

**Figure 1**

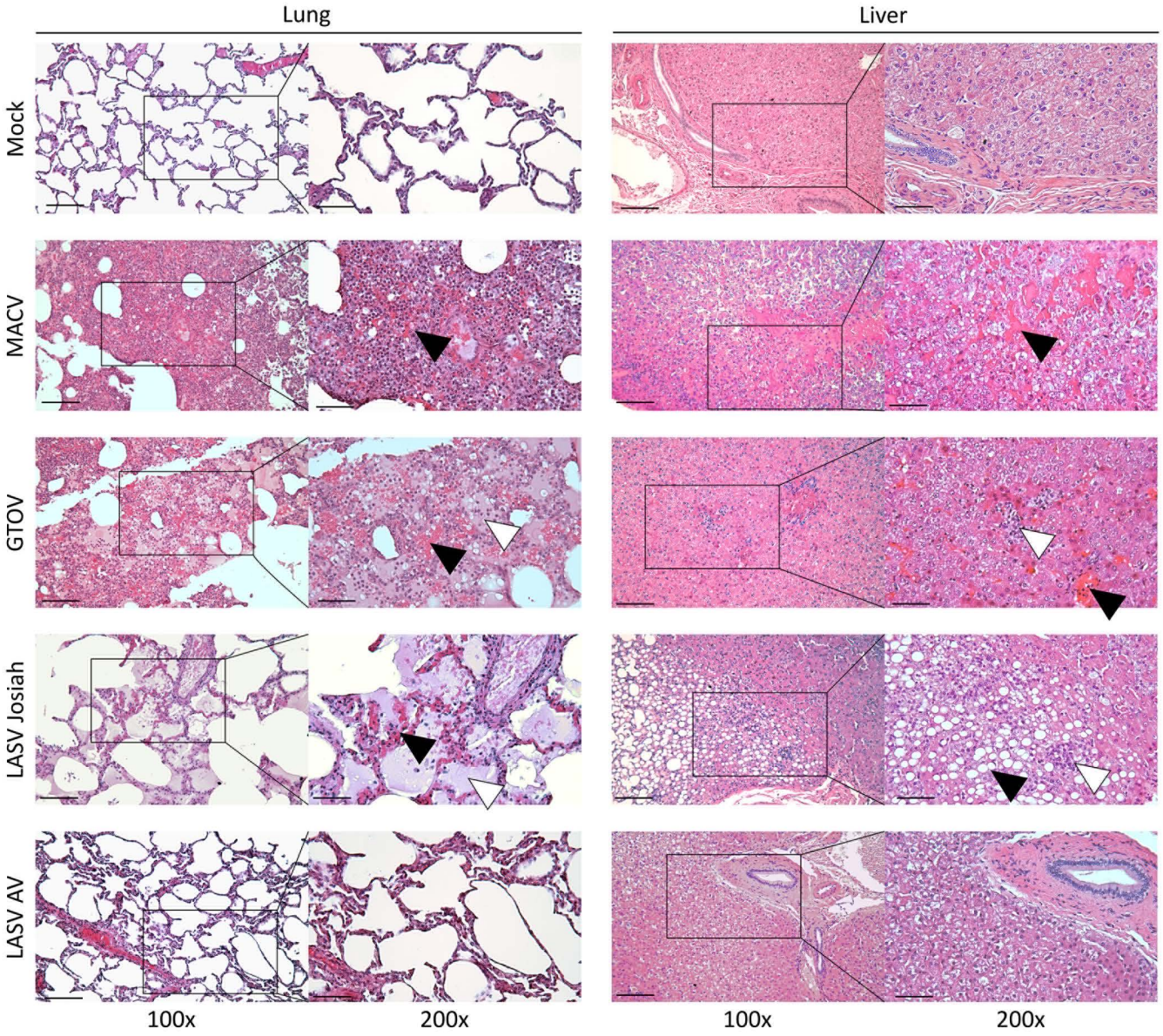
Lung
Liver
Mock
MACV
GTOV
LASV Josiah
LASV AV
100x
200x
100x
200x

**Figure 2**

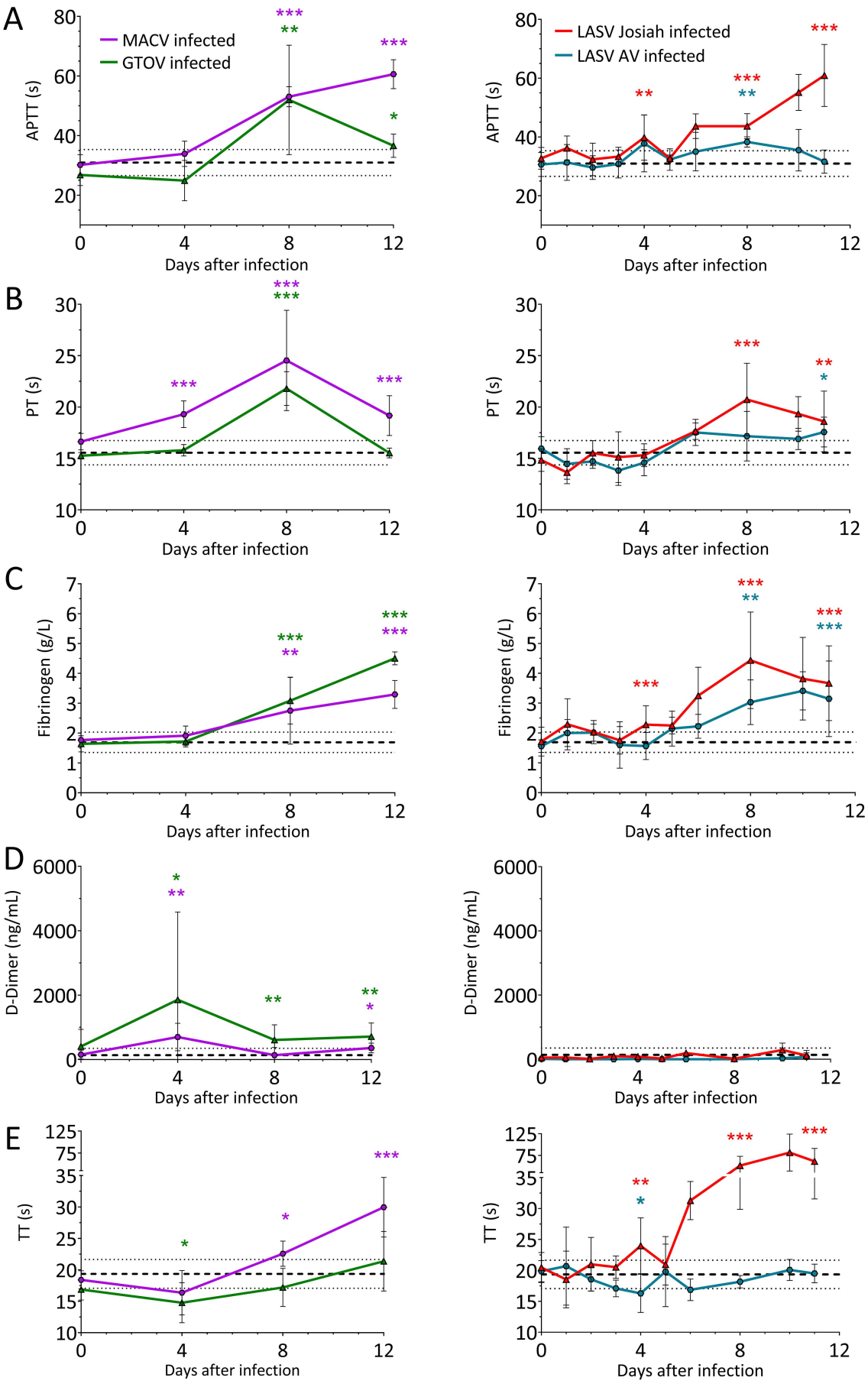
A
APTT (s)
MACV infected
GTOV infected
LASV Josiah infected
LASV AV infected
Days after infection
B
PT (s)
Days after infection
C
Fibrinogen (g/L)
Days after infection
D
D-Dimer (ng/mL)
Days after infection
E
TT (s)
Days after infection

**Figure 3**

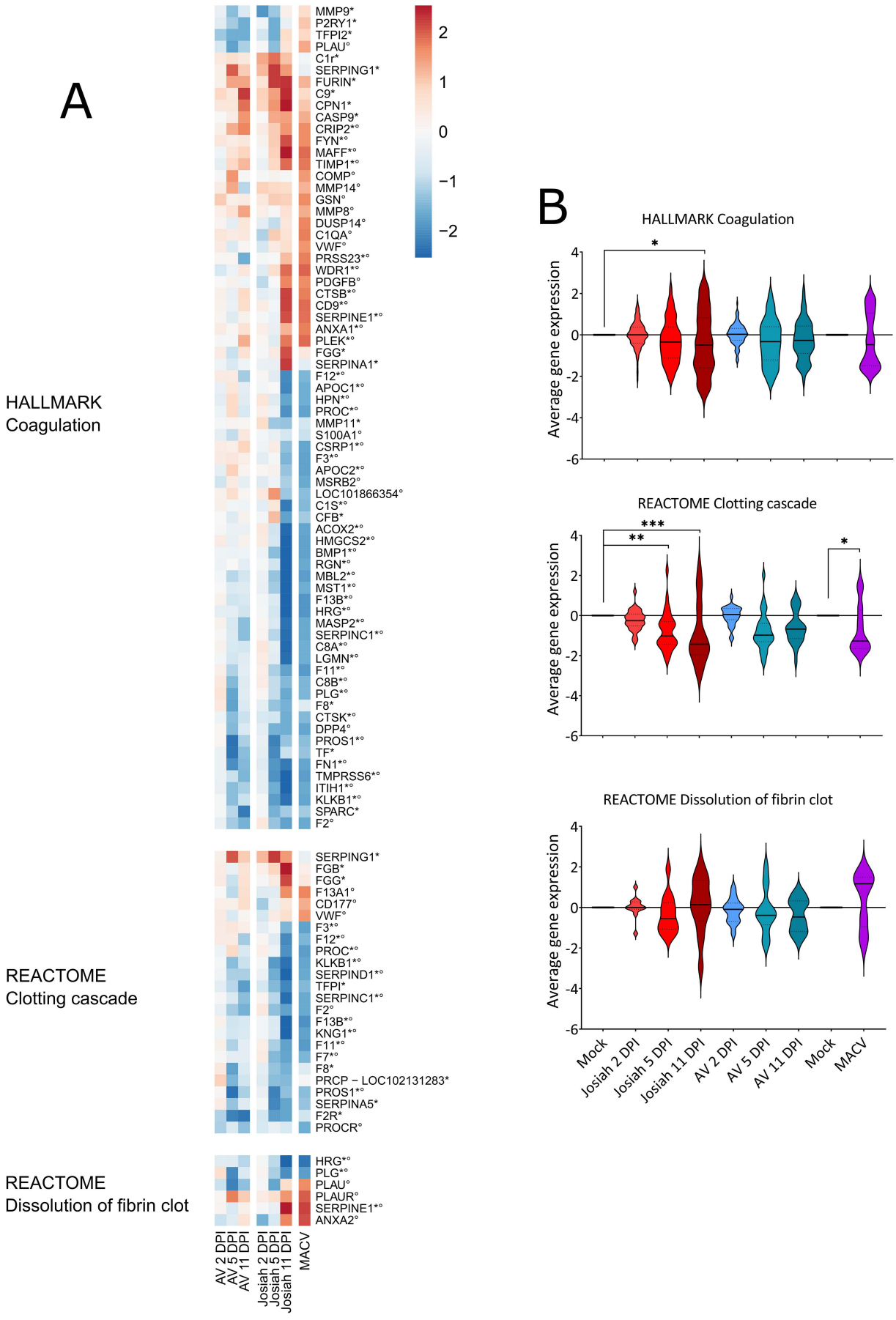
A
HALLMARK
Coagulation
REACTOME
Clotting cascade
REACTOME
Dissolution of fibrin clot
MMP9*
P2RY1*
TFPI2*
PLAU°
C1r*
SERPING1*
FURIN*
C9*
CPN1*
CASP9*
CRIP2*°
FYN*°
MAFF*°
TIMP1*°
COMP°
MMP14°
GSN°
MMP8°
DUSP14°
C1QA°
VWF°
PRSS23*°
WDR1*°
PDGFB°
CTSB*°
CD9*°
SERPINE1*°
ANXA1*°
PLEK*°
FGG*
SERPINA1*
F12*°
APOC1*°
HPN*°
PROC*°
MMP11*
S100A1°
CSRP1*°
F3*°
APOC2*°
MSRB2°
LOC101866354°
C1S*°
CFB*
ACOX2*°
HMGCS2*°
BMP1*°
RGN*°
MBL2*°
MST1*°
F13B*°
HRG*°
MASP2*°
SERPINC1*°
C8A*°
LGMN*°
F11*°
C8B*°
PLG*°
F8*
CTSK*°
DPP4°
PROS1*°
TF*
FN1*°
TMPRSS6*°
ITIH1*°
KLKB1*°
SPARC*
F2°
2
1
0
−1
−2
SERPING1*
FGB*
FGG*
F13A1°
CD177°
VWF°
F3*°
F12*°
PROC*°
KLKB1*°
SERPIND1*°
TFPI*
SERPINC1*°
F2°
F13B*°
KNG1*°
F11*°
F7*°
F8*
PRCP – LOC102131283*
PROS1*°
SERPINA5*
F2R*
PROCR°
HRG*°
PLG*°
PLAU°
PLAUR°
SERPINE1*°
ANXA2°
AV 2 DPI
AV 5 DPI
AV 11 DPI
Josiah 2 DPI
Josiah 5 DPI
Josiah 11 DPI
MACV
B
HALLMARK Coagulation
REACTOME Clotting cascade
REACTOME Dissolution of fibrin clot
Average gene expression
Mock
Josiah 2 DPI
Josiah 5 DPI
Josiah 11 DPI
AV 2 DPI
AV 5 DPI
AV 11 DPI
Mock
MACV

**Figure 4**

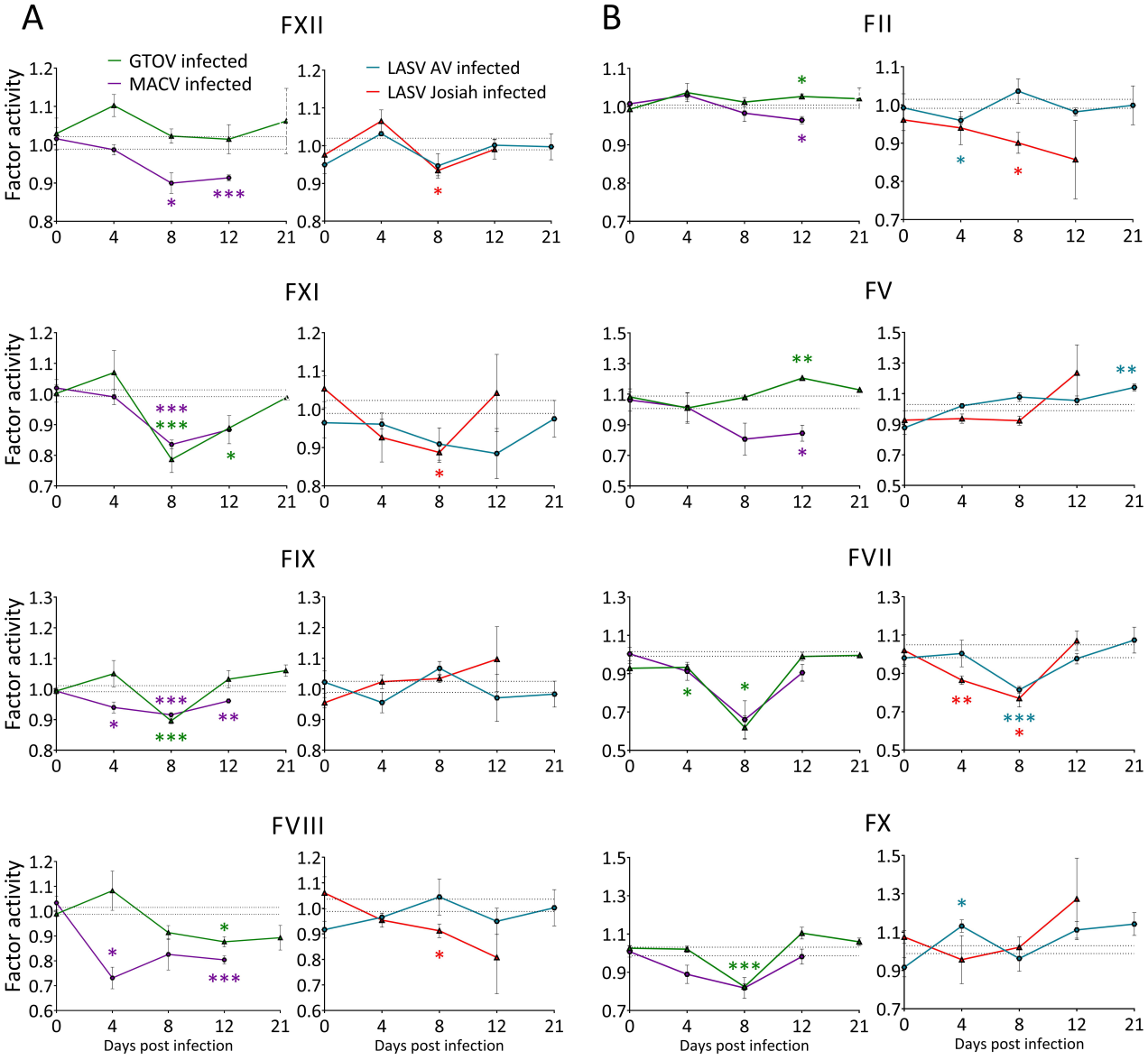
A
B
FXII
FII
FXI
FV
FIX
FVII
FVIII
FX
GTOV infected
MACV infected
LASV AV infected
LASV Josiah infected
Factor activity
Days post infection

**Figure 5**

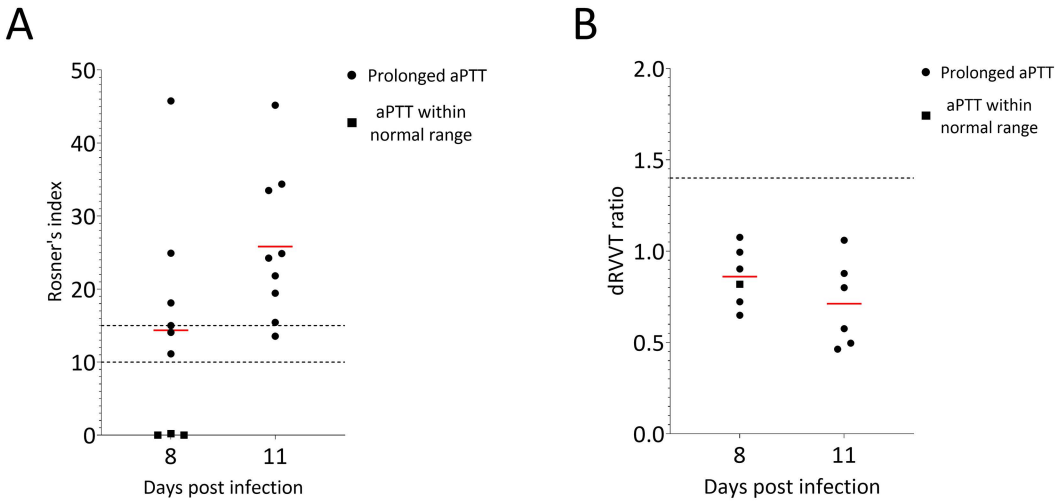
A
Rosner's index
50
40
30
20
10
0
8
11
Days post infection
Prolonged aPTT
aPTT within normal range
B
dRVVT ratio
2.0
1.5
1.0
0.5
0.0
8
11
Days post infection
Prolonged aPTT
aPTT within normal range

**Figure 6**

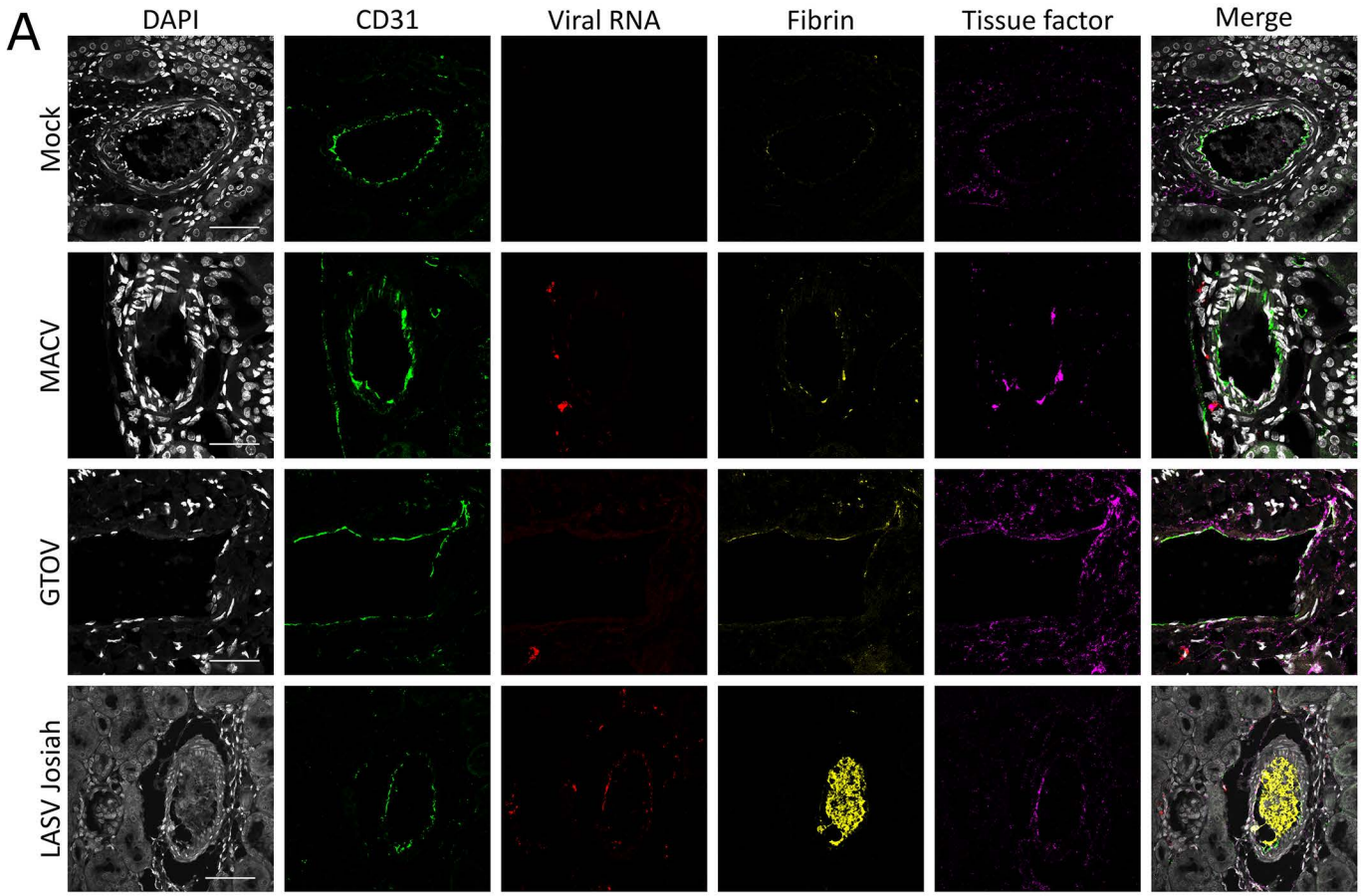
A
DAPI
CD31
Viral RNA
Fibrin
Tissue factor
Merge
Mock
MACV
GTOV
LASV Josiah

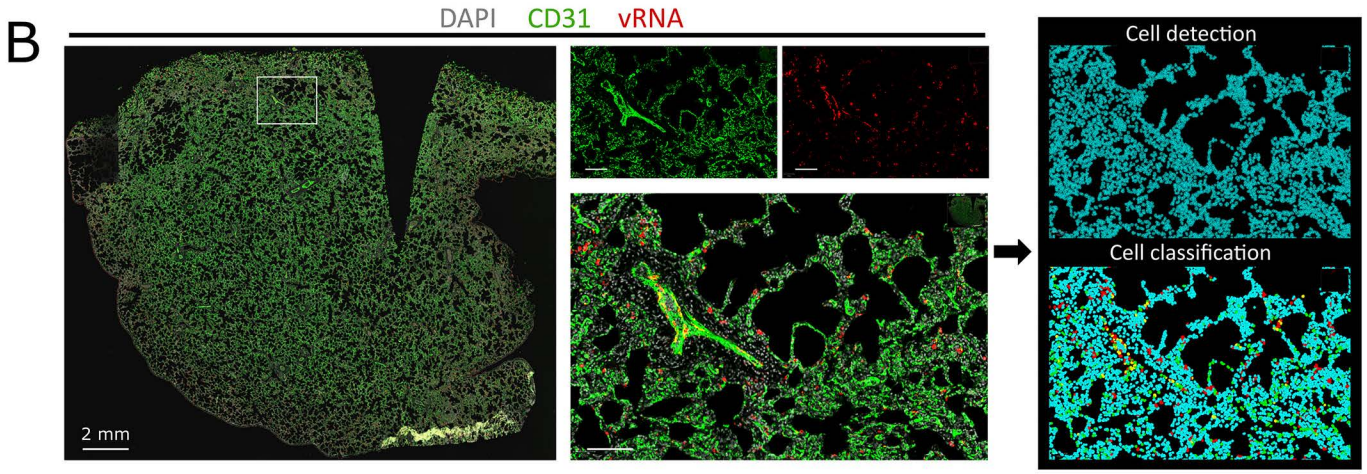
B
DAPI CD31 vRNA
2 mm
Cell detection
Cell classification

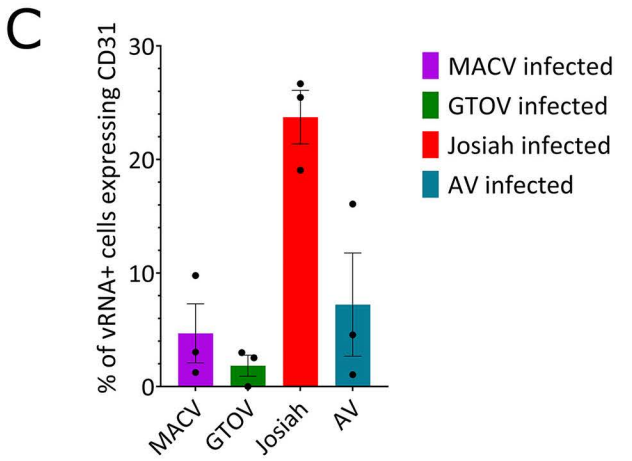
C
% of vRNA+ cells expressing CD31
30
20
10
0
MACV
GTOV
Josiah
AV
MACV infected
GTOV infected
Josiah infected
AV infected

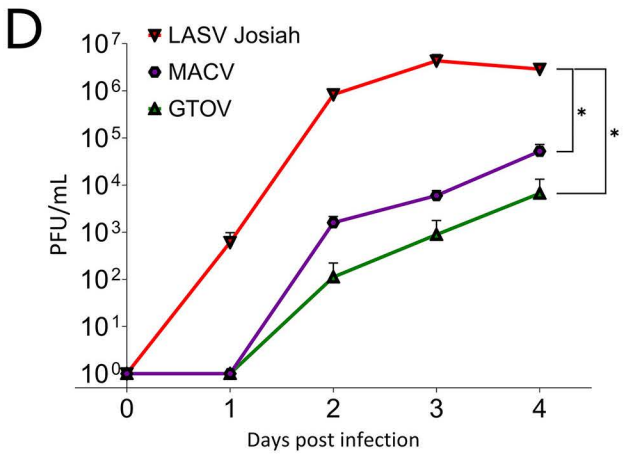
D
LASV Josiah
MACV
GTOV
PFU/mL
Days post infection
*
*

**Figure 7**

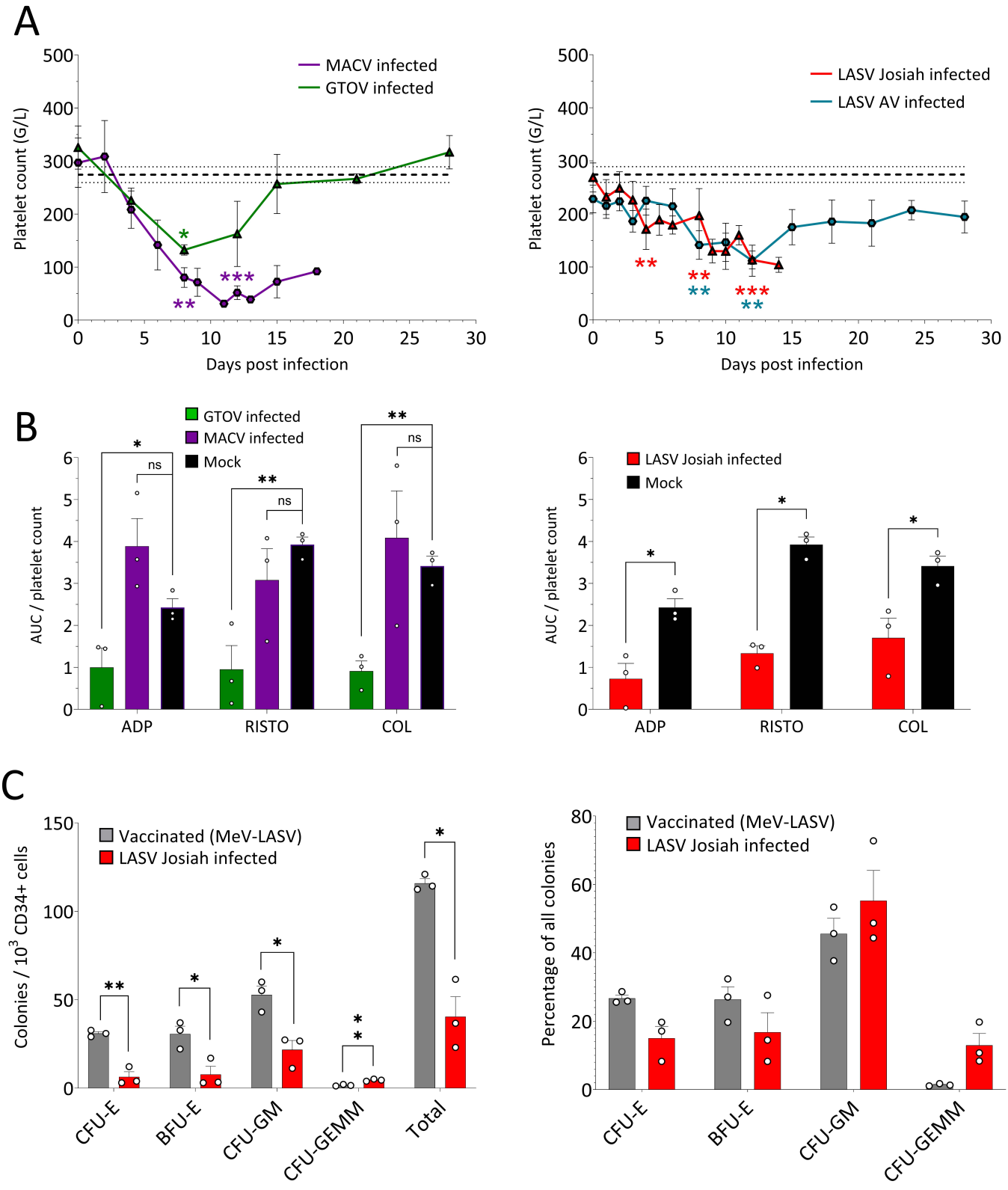
A
MACV infected
GTOV infected
Platelet count (G/L)
Days post infection
LASV Josiah infected
LASV AV infected
B
GTOV infected
MACV infected
Mock
AUC / platelet count
ADP
RISTO
COL
ns
LASV Josiah infected
Mock
C
Vaccinated (MeV-LASV)
LASV Josiah infected
Colonies / 10^3 CD34+ cells
CFU-E
BFU-E
CFU-GM
CFU-GEMM
Total
Percentage of all colonies

## Supplementary Table 1

| CONDITION | N | CLINICAL SIGNS (DAY OF ONSET) | | | | | MORTALITY RATE | MTD | GROSS PATHOLOGY |
|---|---|---|---|---|---|---|---|---|---|
| | | Non-specific | Digestive | Neurological | Hemorrhagic | Percentage of animals with hemorrhagic signs | | | |
| MACV-INFECTED | 6 | Hyperthermia (3), asthenia (7), dehydration (2) | Diarrhea (8) | Ataxia, tremor, prostration (8) | Epistaxis (11), petechiae (18), melena (12), hematochezia (11) | 83% | 100% | 13.5 ± 1.0 | **Pulmonary hemorrhage**, **digestive tract hemorrhage**, focal hepatic ischemia and necrosis, **peritoneal effusion**, pleural adhesions, **subdural cerebral hemorrhage**, **midbrain and cerebellar hemorrhages** |
| GTOV-INFECTED | 3 | Hyperthermia (4), asthenia (7), anorexia (4) | Diarrhea (8) | Ataxia, tremor, prostration (10) | Melena (12), hematochezia (7) | 100 % | 33% | 14 | **Pulmonary hemorrhage**, focal hepatic inflammatory lesions, **subdural cerebral hemorrhage**, **peritoneal effusion, midbrain and cerebellar hemorrhages**, lymphadenopathy |
| LASV JOSIAH-INFECTED | 15 | Hyperthermia (2), asthenia (5), anorexia (4) | Diarrhea (4) | Ataxia & tremor & prostration (10) | Epistaxis (10), petechiae (11) | 55% | 100% | 12.3 ± 0.6 | **Peritoneal effusion**, hepatic steatosis, focal hepatic and pulmonary ischemia and necrosis |
| LASV AV-INFECTED | 9 | Hyperthermia (2), anorexia (6) | Diarrhea (5) | | | 0% | 0% | | |

## Supplementary Table 2

| Days post infection | Leukocytes (G/L) | | Lymphocytes ($x10^3/\mu L$) | | Monocytes ($x10^3/\mu L$) | | Neutrophils ($x10^3/\mu L$) | | Red blood cells ($x10^6/\mu L$) | | MCV (fL) | | MCH (pg) | | MCHC (g/dL) | | Hgb (g/dL) | | MPV (fL) | |
|---|---|---|---|---|---|---|---|---|---|---|---|---|---|---|---|---|---|---|---|---|
| MACV | Mean | SD | Mean | SD | Mean | SD | Mean | SD | Mean | SD | Mean | SD | Mean | SD | Mean | SD | Mean | SD | Mean | SD |
| 0 | 8,4 | 0,9 | 5,1 | 0,5 | 0,8 | 0,5 | 1,7 | 1,0 | 6,6 | 0,6 | 68,9 | 4,0 | 16,8 | 1,6 | 24,5 | 1,9 | 11,0 | 0,7 | 9,3 | 1,3 |
| 4 | 3,3 | 0,9 | 1,6 | 0,3 | 0,3 | 0,1 | 1,1 | 0,4 | 6,3 | 0,7 | 68,3 | 4,0 | 16,7 | 1,6 | 24,5 | 1,7 | 10,5 | 0,8 | 9,2 | 1,2 |
| 8 | 1,9 | 0,2 | 1,0 | 0,2 | 0,2 | 0,1 | 0,7 | 0,3 | 5,8 | 0,6 | 68,5 | 5,2 | 17,0 | 1,2 | 24,9 | 0,2 | 9,9 | 0,9 | 8,9 | 0,7 |
| 12 | 3,1 | 1,5 | 1,8 | 0,8 | 0,2 | 0,1 | 1,0 | 0,6 | 5,1 | 0,8 | 67,7 | 4,3 | 16,0 | 1,9 | 23,6 | 2,0 | 8,1 | 1,4 | 7,7 | 1,2 |
| Days post infection | Leukocytes (G/L) | | Lymphocytes ($x10^3/\mu L$) | | Monocytes ($x10^3/\mu L$) | | Neutrophils ($x10^3/\mu L$) | | RED blood cells ($x10^6/\mu L$) | | MCV (fL) | | MCH (pg) | | MCHC (g/dL) | | Hgb (g/dL) | | MPV (fL) | |
| GTOV | Mean | SD | Mean | SD | Mean | SD | Mean | SD | Mean | SD | Mean | SD | Mean | SD | Mean | SD | Mean | SD | Mean | SD |
| 0 | 10,6 | 3,6 | 5,1 | 0,9 | 1,7 | 0,7 | 2,3 | 1,7 | 6,5 | 0,6 | 69,1 | 2,6 | 18,1 | 1,4 | 26,2 | 1,2 | 11,6 | 0,6 | 9,6 | 0,5 |
| 4 | 5,7 | 0,5 | 3,0 | 0,8 | 1,0 | 0,2 | 1,7 | 0,6 | 6,3 | 0,4 | 69,1 | 2,1 | 17,5 | 1,1 | 25,4 | 1,0 | 10,9 | 0,1 | 9,4 | 1,1 |
| 8 | 3,4 | 0,6 | 1,4 | 0,1 | 0,5 | 0,2 | 1,5 | 0,5 | 5,6 | 0,4 | 68,2 | 2,6 | 17,0 | 1,4 | 24,8 | 1,2 | 9,5 | 0,2 | 9,6 | 0,8 |
| 12 | 3,6 | 0,4 | 1,8 | 0,6 | 0,3 | 0,1 | 1,5 | 0,2 | 5,6 | 0,4 | 67,5 | 2,3 | 16,8 | 0,8 | 24,9 | 0,6 | 9,4 | 0,5 | 10,6 | 0,9 |
| 21 | 8,2 | 4,2 | 6,1 | 3,2 | 0,7 | 0,6 | 1,4 | 0,4 | 4,8 | 0,1 | 68,7 | 1,3 | 17,6 | 0,1 | 25,7 | 0,4 | 8,4 | 0,1 | 10,1 | 1,0 |
| 28 | 6,2 | 2,3 | 4,1 | 2,3 | 0,5 | 0,1 | 1,6 | 0,1 | 4,7 | 0,4 | 67,2 | 0,1 | 17,8 | 0,1 | 26,5 | 0,4 | 8,3 | 0,6 | 9,3 | 1,2 |
| Days post infection | Leukocytes (G/L) | | Lymphocytes ($x10^3/\mu L$) | | Monocytes ($x10^3/\mu L$) | | Neutrophils ($x10^3/\mu L$) | | RED blood cells ($x10^6/\mu L$) | | MCV (fL) | | MCH (pg) | | MCHC (g/dL) | | Hgb (g/dL) | | MPV (fL) | |
| Mock | Mean | SD | Mean | SD | Mean | SD | Mean | SD | Mean | SD | Mean | SD | Mean | SD | Mean | SD | Mean | SD | Mean | SD |
| 0 | 5,4 | 2,2 | 2,4 | 1,1 | 0,3 | 0,1 | 2,5 | 0,9 | 5,5 | 0,6 | 71,0 | 3,0 | 21,9 | 3,4 | 30,9 | 3,4 | 12,1 | 0,6 | 7,6 | 0,2 |
| 4 | 6,3 | 1,2 | 2,2 | 0,5 | 0,4 | 0,2 | 2,3 | 0,6 | 3,9 | 1,1 | 71,0 | 2,9 | 26,6 | 4,8 | 37,5 | 5,6 | 10,4 | 0,4 | 6,9 | 0,9 |
| 8 | 4,5 | 2,9 | 0,8 | 1,3 | 0,2 | 0,2 | 3,3 | 1,3 | 4,2 | 1,0 | 71,1 | 2,7 | 23,6 | 3,7 | 33,2 | 4,2 | 10,0 | 0,2 | 6,8 | 0,8 |
| 12 | 7,9 | 1,8 | 2,7 | 0,4 | 0,4 | 0,1 | 1,4 | 1,0 | 4,4 | 1,1 | 71,2 | 2,0 | 21,1 | 2,7 | 29,6 | 3,1 | 9,3 | 0,6 | 7,5 | 0,3 |
| 21 | 6,3 | 1,3 | 2,0 | 1,2 | 0,3 | 0,2 | 3,9 | 1,7 | 3,9 | 1,1 | 71,0 | 2,1 | 24,5 | 4,1 | 34,5 | 5,1 | 9,5 | 0,3 | 7,1 | 0,7 |
| 28 | 4,9 | 1,0 | 1,9 | 1,2 | 0,2 | 0,2 | 1,2 | 0,2 | 3,5 | 1,3 | 72,6 | 2,9 | 28,6 | 6,5 | 39,4 | 7,9 | 10,1 | 0,1 | 7,3 | 0,6 |
| Days post infection | Leukocytes (G/L) | | Lymphocytes ($x10^3/\mu L$) | | Monocytes ($x10^3/\mu L$) | | Neutrophils ($x10^3/\mu L$) | | RED blood cells ($x10^6/\mu L$) | | MCV (fL) | | MCH (pg) | | MCHC (g/dL) | | Hgb (g/dL) | | MPV (fL) | |
| AV | Mean | SD | Mean | SD | Mean | SD | Mean | SD | Mean | SD | Mean | SD | Mean | SD | Mean | SD | Mean | SD | Mean | SD |
| 0 | 4,7 | 2,3 | 2,1 | 0,9 | 0,3 | 0,1 | 1,3 | 1,1 | 5,0 | 0,3 | 68,3 | 1,4 | 25,0 | 1,3 | 36,7 | 1,7 | 12,4 | 0,1 | 7,6 | 0,3 |
| 4 | 4,1 | 1,7 | 1,5 | 0,2 | 0,2 | 0,1 | 1,9 | 1,0 | 4,5 | 0,1 | 67,5 | 1,4 | 24,5 | 0,5 | 36,2 | 0,2 | 10,9 | 0,3 | 7,9 | 0,4 |
| 8 | 2,7 | 0,9 | 1,0 | 0,4 | 0,2 | 0,1 | 1,0 | 0,4 | 3,9 | 0,2 | 67,2 | 0,7 | 24,8 | 1,7 | 36,8 | 2,9 | 9,7 | 0,4 | 7,8 | 0,7 |
| 12 | 5,0 | 1,3 | 2,2 | 0,5 | 0,3 | 0,1 | 0,8 | 0,8 | 3,2 | 1,1 | 70,9 | 9,1 | 32,0 | 17,8 | 43,5 | 17,3 | 8,7 | 0,3 | 8,9 | 0,8 |
| 21 | 9,6 | 1,9 | 4,7 | 1,5 | 0,6 | 0,1 | 1,9 | 1,1 | 3,8 | 0,7 | 67,8 | 1,3 | 25,3 | 0,9 | 37,4 | 0,8 | 9,7 | 1,4 | 7,4 | 0,6 |
| 28 | 7,5 | 1,9 | 3,3 | 0,5 | 0,4 | 0,2 | 2,4 | 0,8 | 3,7 | 0,2 | 70,0 | 1,8 | 27,1 | 0,4 | 38,7 | 1,2 | 10,0 | 0,3 | 6,8 | 0,7 |
| Days post infection | Leukocytes (G/L) | | Lymphocytes ($x10^3/\mu L$) | | Monocytes ($x10^3/\mu L$) | | Neutrophils ($x10^3/\mu L$) | | RED blood cells ($x10^6/\mu L$) | | MCV (fL) | | MCH (pg) | | MCHC (g/dL) | | Hgb (g/dL) | | MPV (fL) | |
| Josiah | Mean | SD | Mean | SD | Mean | SD | Mean | SD | Mean | SD | Mean | SD | Mean | SD | Mean | SD | Mean | SD | Mean | SD |
| 0 | 8,4 | 3,1 | 4,4 | 1,4 | 0,5 | 0,3 | 2,9 | 1,5 | 7,0 | 1,2 | 65,5 | 3,9 | 18,0 | 2,7 | 27,6 | 4,4 | 12,4 | 0,7 | 8,5 | 0,7 |
| 4 | 7,2 | 2,6 | 2,1 | 0,8 | 0,4 | 0,2 | 4,0 | 1,9 | 6,2 | 0,5 | 67,0 | 1,0 | 18,6 | 1,1 | 27,8 | 1,6 | 11,4 | 0,5 | 8,6 | 0,9 |
| 8 | 3,2 | 1,2 | 1,2 | 0,3 | 0,2 | 0,1 | 1,6 | 0,9 | 5,4 | 0,8 | 67,4 | 1,5 | 17,7 | 0,4 | 26,3 | 0,4 | 9,6 | 1,3 | 8,6 | 0,7 |
| 12 | 8,1 | 4,8 | 3,0 | 1,4 | 0,4 | 0,3 | 3,6 | 2,5 | 5,8 | 1,1 | 65,3 | 4,6 | 16,8 | 2,4 | 25,8 | 4,0 | 9,5 | 0,9 | 8,6 | 0,8 |

**Suppl Fig 1**

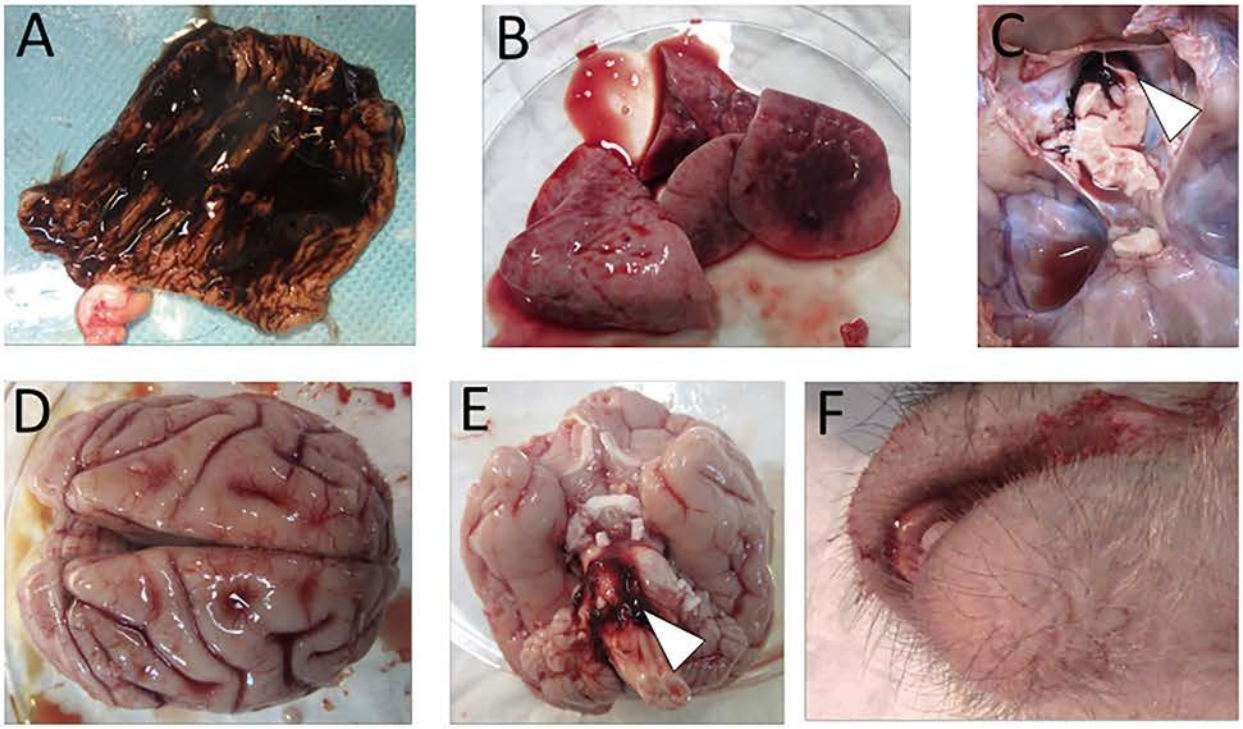

**Suppl Fig 2**

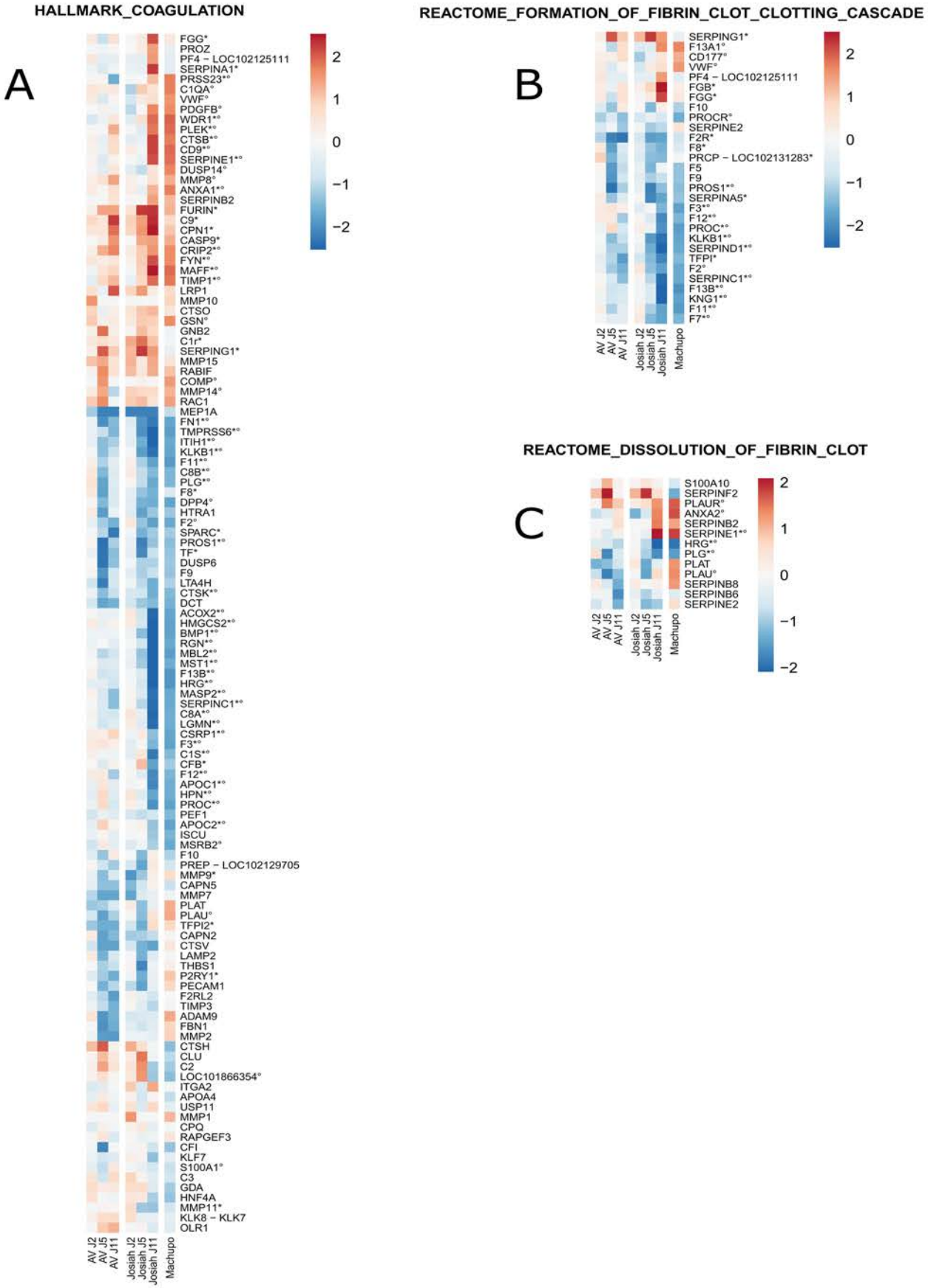
A
HALLMARK_COAGULATION
FGG*
PROZ
PF4 – LOC102125111
SERPINA1*
PRSS23*°
C1QA°
VWF°
PDGFB°
WDR1*°
PLEK*°
CTSB*°
CD9*°
SERPINE1*°
DUSP14°
MMP8°
ANXA1*°
SERPINB2
FURIN*
C9*
CPN1*
CASP9*
CRIP2*°
FYN*°
MAFF*°
TIMP1*°
LRP1
MMP10
CTSO
GSN°
GNB2
C1r*
SERPING1*
MMP15
RABIF
COMP°
MMP14°
RAC1
MEP1A
FN1*°
TMPRSS6*°
ITIH1*°
KLKB1*°
F11*°
C8B*°
PLG*°
F8*
DPP4°
HTRA1
F2°
SPARC*
PROS1*°
TF*
DUSP6
F9
LTA4H
CTSK*°
DCT
ACOX2*°
HMGCS2*°
BMP1*°
RGN*°
MBL2*°
MST1*°
F13B*°
HRG*°
MASP2*°
SERPINC1*°
C8A*°
LGMN*°
CSRP1*°
F3*°
C1S*°
CFB*
F12*°
APOC1*°
HPN*°
PROC*°
PEF1
APOC2*°
ISCU
MSRB2°
F10
PREP – LOC102129705
MMP9*
CAPN5
MMP7
PLAT
PLAU°
TFPI2*
CAPN2
CTSV
LAMP2
THBS1
P2RY1*
PECAM1
F2RL2
TIMP3
ADAM9
FBN1
MMP2
CTSH
CLU
C2
LOC101866354°
ITGA2
APOA4
USP11
MMP1
CPQ
RAPGEF3
CFI
KLF7
S100A1°
C3
GDA
HNF4A
MMP11*
KLK8 – KLK7
OLR1
2
1
0
−1
−2
AV J2
AV J5
AV J11
Josiah J2
Josiah J5
Josiah J11
Machupo
B
REACTOME_FORMATION_OF_FIBRIN_CLOT_CLOTTING_CASCADE
SERPING1*
F13A1°
CD177°
VWF°
PF4 – LOC102125111
FGB*
FGG*
F10
PROCR°
SERPINE2
F2R*
F8*
PRCP – LOC102131283*
F5
F9
PROS1*°
SERPINA5*
F3*°
F12*°
PROC*°
KLKB1*°
SERPIND1*°
TFPI*
F2°
SERPINC1*°
F13B*°
KNG1*°
F11*°
F7*°
2
1
0
−1
−2
AV J2
AV J5
AV J11
Josiah J2
Josiah J5
Josiah J11
Machupo
C
REACTOME_DISSOLUTION_OF_FIBRIN_CLOT
S100A10
SERPINF2
PLAUR°
ANXA2°
SERPINB2
SERPINE1*°
HRG*°
PLG*°
PLAT
PLAU°
SERPINB8
SERPINB6
SERPINE2
2
1
0
−1
−2
AV J2
AV J5
AV J11
Josiah J2
Josiah J5
Josiah J11
Machupo

**Suppl Fig 3**

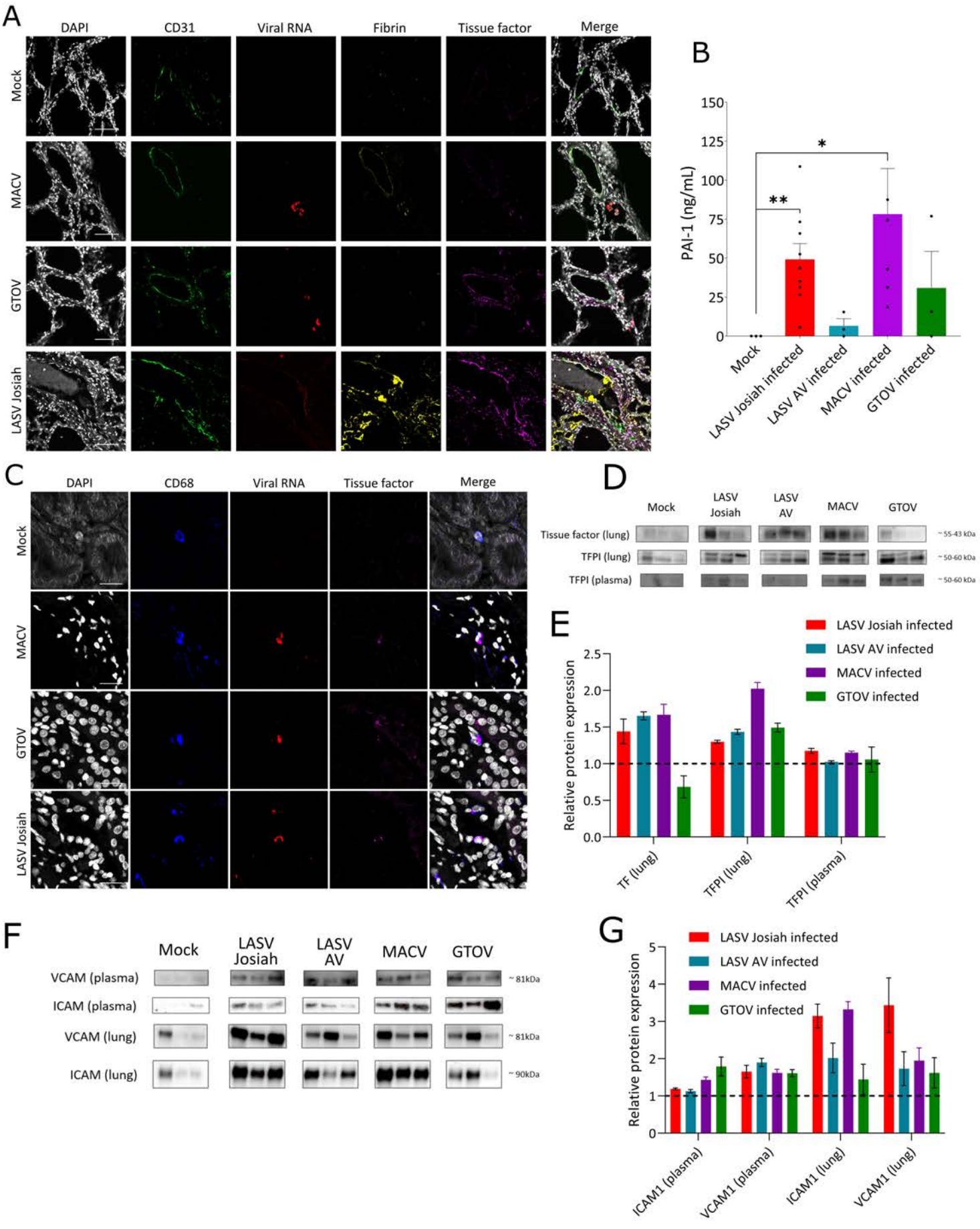
A
DAPI
CD31
Viral RNA
Fibrin
Tissue factor
Merge
Mock
MACV
GTOV
LASV Josiah
B
PAI-1 (ng/mL)
150
125
100
75
50
25
0
*
**
Mock
LASV Josiah infected
LASV AV infected
MACV infected
GTOV infected
C
DAPI
CD68
Viral RNA
Tissue factor
Merge
Mock
MACV
GTOV
LASV Josiah
D
Mock
LASV Josiah
LASV AV
MACV
GTOV
Tissue factor (lung)
TFPI (lung)
TFPI (plasma)
~55-43 kDa
~50-60 kDa
~50-60 kDa
E
LASV Josiah infected
LASV AV infected
MACV infected
GTOV infected
Relative protein expression
2.5
2.0
1.5
1.0
0.5
0.0
TF (lung)
TFPI (lung)
TFPI (plasma)
F
Mock
LASV Josiah
LASV AV
MACV
GTOV
VCAM (plasma)
ICAM (plasma)
VCAM (lung)
ICAM (lung)
~81kDa
~81kDa
~90kDa
G
LASV Josiah infected
LASV AV infected
MACV infected
GTOV infected
Relative protein expression
5
4
3
2
1
0
ICAM1 (plasma)
VCAM1 (plasma)
ICAM1 (lung)
VCAM1 (lung)

**Suppl Fig 4**

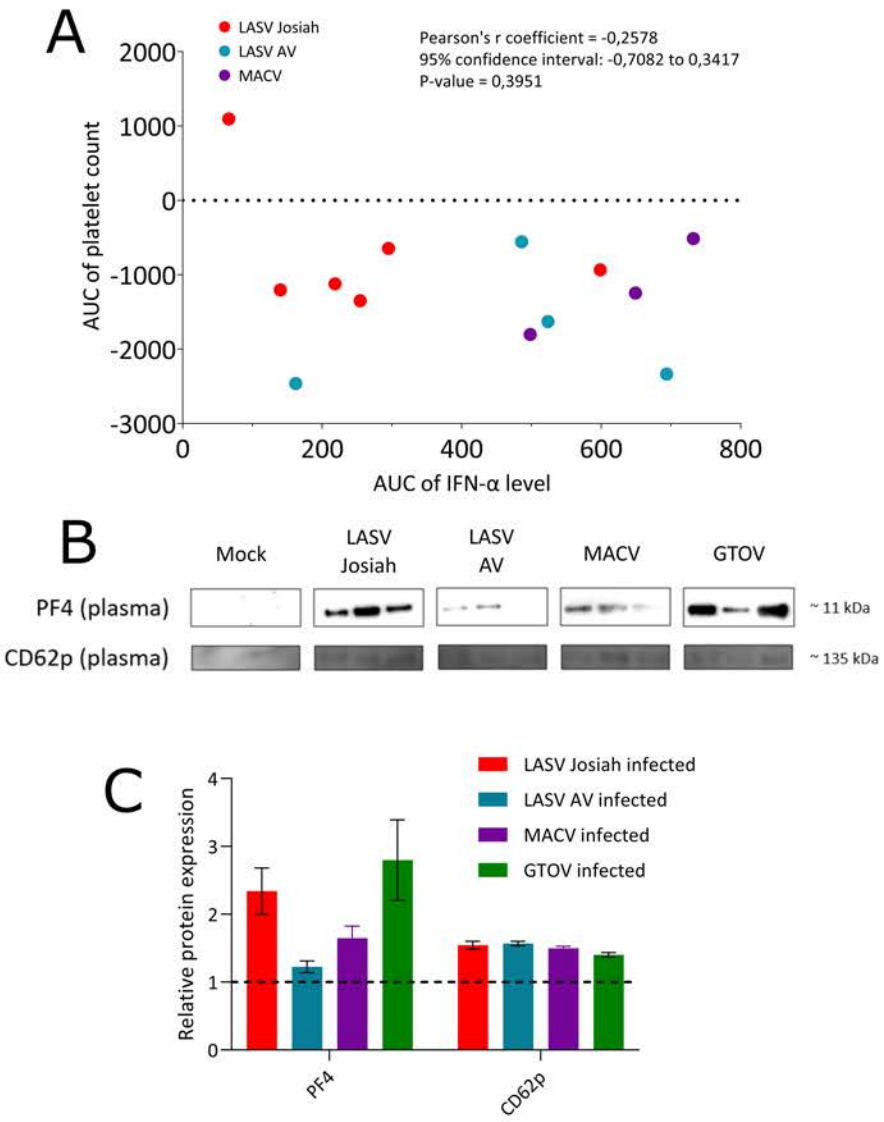
A
LASV Josiah
LASV AV
MACV
Pearson's r coefficient = -0,2578
95% confidence interval: -0,7082 to 0,3417
P-value = 0,3951
AUC of platelet count
AUC of IFN-α level
B
Mock
LASV Josiah
LASV AV
MACV
GTOV
PF4 (plasma)
CD62p (plasma)
~ 11 kDa
~ 135 kDa
C
LASV Josiah infected
LASV AV infected
MACV infected
GTOV infected
Relative protein expression
PF4
CD62p

**Supplementary Table 1. Clinical follow-up and post-mortem examination of infected cynomolgus macaques**. The clinical signs, mortality and macroscopic pathology of all animals included in this study is recapitulated. Hyperthermia corresponds to a minimal 1°C increase in body temperature. Asthenia is based on a decreased interaction with the environment. The day of onset is the earliest day post-infection on which the symptom was observed. The percentages of animals with hemorrhagic manifestations, mortality rates and mean times of death were calculated excluding precociously euthanized animals. The pathologic findings related to hemostasis defects or increased vascular permeability are in bold.

**Supplementary Table 2. Hematological parameters changes following infection.** Means and standard deviations of a minimum of 3 animals and a maximum of 15 animals depending on the virus and the day of sampling. MCV = Mean Corpuscular Volume; MCH = Mean Corpuscular Hemoglobin; MCHC = Mean Corpuscular Hemoglobin Concentration; Hgb = Hemoglobin; MPV = Mean Platelet Volume.

**Supplementary figure 1. Macroscopic hemorrhagic manifestations at necropsy. A.** Resected part of the small intestine containing digested blood, manifesting an active hemorrhage in the upper gastro-intestinal tract. **B.** Resected lung lobes with large areas of hemorrhage and necrosis. **C.** Upper view of the base of the skull after removal of the brain and cerebellum. Arrowhead indicates coagulated blood compressing the brain stem inside the foramen magnum. **D.** Meningeal congestion and moderate hematoma at the surface of the brain cortex. **E.** Resected brain, cerebellum and bran stem. Arrowhead points toward a hemorrhage at the anterior part of the cerebellum around the pons and medulla oblongata. **F.** Gum bleed.

**Supplementary figure 2. Transcriptomic analysis of pathways associated with hemostasis in the liver of animals infected with LASV Josiah, LASV AV or MACV. A.** Gene set HALLMARK Coagulation. **B.** Gene set REACTOME Dissolution of fibrin clot. **C.** Gene set REACTOME Formation of fibrin clot & clotting cascade. Average gene expression of each condition relative to mock is color-coded on a blue-to-red scale. Gene names were annotated regarding their differential expression status: asterisk refers to genes significant in the mock-AV-Josiah dataset while degree symbols refer to genes significant in the Machupo dataset.

**Supplementary figure 3. Viral tropism in the lungs of infected animals and tissue factor expression in infected monocytes. A.** Multiplex immunofluorescence and ISH staining of lung sections from infected or mock-infected animals. Single channel images of DAPI, CD31 (endothelial cells), fibrin, viral RNA and tissue factor are shown as well as their merge. Images are representative of observations made in three separate animals for each condition. Scale bar corresponds to 50 µm. **B.** Multiplex immunofluorescence and ISH staining in kidney sections showing expression of tissue factor in infected or uninfected monocytes. Scale bar corresponds to 12.5 µm. **C.** Plasmatic levels of Plasminogen Activator Inhibitor 1 (PAI-1) in infected animals at 11 days post infection for LASV AV and LASV Josiah or at the day of euthanasia for Mock (28 DPI) MACV (11, 11, 12, 13, 15 and 18 DPI) and GTOV (14, 28 and 28 DPI) animals. Number of animals: Mock = 3; LASV Josiah = 9; LASV AV = 3; MACV = 6; GTOV = 3. Asterisks indicate a significant difference according to a two-tailed Mann-Whitney test with one asterisk for $p<0.05$ and two for $p<0.01$. **D and F.** Western blots of plasma samples and lung homogenates of infected animals. Three animals were analyzed for each condition and are presented next to each other. For a given protein target, all samples were treated together during all the protocol. TF was not detected in plasma samples. **E and G.** Mean relative protein expressions evaluated by quantifying signal intensities of the Western Blots in ImageJ and individually dividing them by the mean of mock-infected animals. Intensities were measured only at the expected molecular weight on the membrane. VCAM-1 = Vascular cell adhesion protein 1; ICAM-1 = InterCellular Adhesion Molecule 1; TF= Tissue Factor; TFPI = Tissue Factor Pathway Inhibitor.

**Supplementary figure 4. Putative factors influencing platelet numbers and function. A.** Correlation plot of the Area Under the Curve (AUC) of the IFN-α1 level against the AUC of the platelet count along the course of the infection for 3 animals infected by MACV, 4 animals infected by LASV AV and 6 animals infected by LASV Josiah. A negative AUC for platelet count indicates an overall decrease in platelet count. Data points are color-coded according to the viral strain. The results of a two-tailed Pearson correlation analysis are printed with the graph. B. Western blots of plasma samples and lung homogenates of infected animals. Three animals were analyzed for each condition and are presented next to each other. For a given protein target, all samples were treated together during all the protocol. E and G. Mean relative protein expressions evaluated by quantifying signal intensities of the Western Blots in ImageJ and individually dividing them by the mean of mock-infected animals. Intensities were measured only at the expected molecular weight on the membrane. PF4 = Platelet Factor 4; CD62p = P-selectin.